2026 NASA Human Lander Challenge (HuLC)

PHAT

Peltier-based Hydration Accumulation Terminal

Technical Paper

California Polytechnic State University, San Luis Obispo

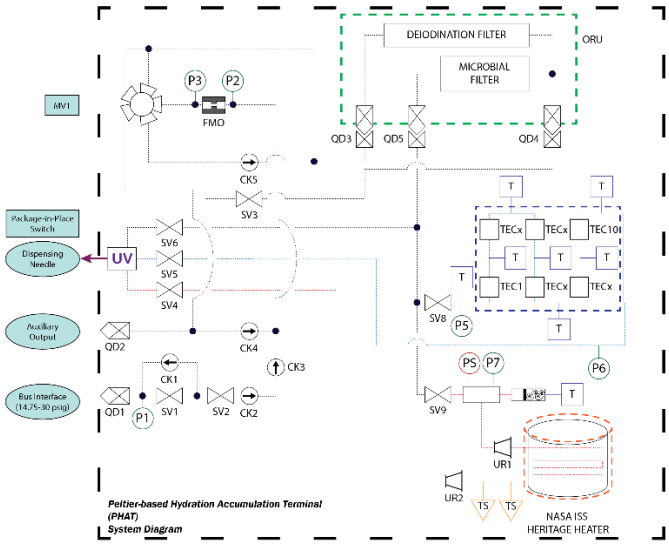

Team Members

Taehoon Lee
Undergraduate, Mechanical Engineering

Sabrina Luo
Undergraduate, Mechanical Engineering

Jenner Mucher
Undergraduate, Mechanical Engineering

Tarsem Pal
Undergraduate, Mechanical Engineering

Ethan Pace
Undergraduate, Mechanical Engineering

Renee Rebolledo
Undergraduate, Mechanical Engineering

Advisor: Dr. John Chen, Professor, Mechanical Engineering

P.H.A.T. — Peltier-based Hydration Accumulation Terminal

California Polytechnic State University, San Luis Obispo

Theme Category, Major Objectives, & Technology

THEME SUBTOPIC

- Crew life support — potable water for long-duration lunar & Mars exploration
- Cold water dispensing absent from all current flight hardware

MAIN OBJECTIVE

- Add cold water capability (<16°C) to the NASA ISS Potable Water Dispenser heritage design using solid-state Peltier cooling.

TECHNICAL APPROACH

- Heritage-first: TRL-9 ISS PWD core preserved; all new risk in modular TEC cold-loop
- 10 × 180 W Peltier modules in sequential stages along 316L SS serpentine pipe at 0.50 L/min
- Liquid heat exchanger hot-side rejection; 40 mm aerogel condensation enclosure
- Dual microbial control: ACTEX deiodination filter + UV-C sterilization module

System Concept & Performance

KEY PERFORMANCE

16°C (60.8°F)
Outlet Temperature
(Target Temp)

421W
Outlet Temperature
(2000W budget)

0.91
System COP
at worst case

WORST CASE
(27°C INLET WATER TEMP)

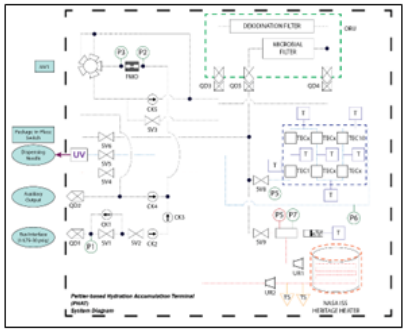

Key Design Details & Innovations

INNOVATIONS

- First spaceflight PWD with TEC cooling — no refrigerants, gravity-independent
- Heat Exchanger hot side makes 10-module config feasible within power budget
- Modular TEC architecture allows crew replacement without special tools
- UV-C sterilization provides microbial-control redundancy during delayed ACTEX replacement

BENCH TESTING

- 2 × 180 W Peltier modules in flow-through config validated sequential thermal model
- Key findings: residence time and hot-side rejection were limiting factors → drove final design

TECHNOLOGY READINESS

Subsystem	TRL
ISS PWD Heritage Core (heater, valves, filters)	9
TEC Modules (spacecraft instrument cooling heritage)	6
SS Pipe / Copper Saddle / Heat Exchanger Cold Loop	3
Integrated P.H.A.T. System	3

Schedule, Costs, & Adoption Path

DEVELOPMENT SCHEDULE

2026-27	2027	2028	2033	2033+
Component Test TEC breadboard; aerogel & UV-C validation	**Subsystem Integration** 10-module array; launch load testing	**ISS Flight Demo** 180-day Express Rack microgravity validation	**HLS Certification** Integration, gloved-hand testing, flight cert	**Flight Ops** Artemis lunar; Mars infusion pathway
→ TRL 5	→ TRL 6	→ TRL 7	→ TRL 8	→ TRL 9

COST ESTIMATE

- $9.21M (2025)

MISSION SCALABILITY

- **Moon (30-day):** Filter lifetime, UV-C LED rated life, and TEC cycle accumulation all exceed 30-day operational requirements.
- **Mars (1,200-day):** Filters need periodic swapping; the UV sterilizer keeps water safe in the meantime. If a cooling module fails, the crew replaces just that piece without tools.

Table of Contents

Table of Acronyms

ACTEX	Activated Carbon Ion Exchange
CER	Cost Estimating Relationship
COP	Coefficient of Performance
DT&E	Development, Test, and Evaluation
ECLSS	Environmental Control and Life Support System
EVA	Extravehicular Activity
HLS	Human Landing System
HuLC	Human Lander Challenge
ISS	International Space Station
NASA	National Aeronautics and Space Administration
PHAT	Peltier-based Hydration Accumulation Terminal
PWD	Potable Water Dispenser
Re	Reynold's Number
TEC	Thermoelectric Cooler
TRL	Technology Readiness Level
UV	Ultraviolet
V&V	Verification and Validation
VDC	Volts Direct Current

1 Executive Summary

PHAT — Peltier-based Hydration Accumulation Terminal — addresses the absence of cold potable water in current spaceflight dispenser architectures while preserving heritage hot and ambient dispensing. The design adds a modular solid-state thermoelectric cold loop to the ISS Potable Water Dispenser architecture rather than replacing the proven core system. Ten TEC stages cool iodinated potable water through a 316L stainless-steel serpentine line to ≤16°C, reject worst-case heat to the spacecraft thermal loop, and use ACTEX plus UV-C for microbial-control redundancy. PHAT provides a low-risk ECLSS upgrade for HLS lunar missions and a scalable Mars-forward crew-water architecture.

2 Project Description

2.1 Challenge and Objectives

Potable-water dispensing is a crew life-support function required for hydration, food rehydration, and beverage preparation. The ISS Potable Water Dispenser (PWD) provides reliable hot and ambient water through a pressure-fed, pump-free architecture designed to avoid free-gas generation in microgravity [1]. However, the ISS PWD does not provide cold potable water, and its hot-water throughput is limited by heater recovery time between consecutive dispenses [1]. NASA-STD-3001 identifies 0-16°C as the required cold potable-water range [2], creating a capability gap for exploration missions where one dispenser may serve the full crew.

PHAT addresses this gap by adding cold-water capability to the ISS PWD architecture without replacing the flight-proven hot and ambient dispensing functions. The design objectives are to deliver ≤16°C potable water under HLS cabin conditions, preserve microgravity-compatible pressure-fed operation, avoid refrigerants and compressor hardware, fit within a rack-scale spacecraft interface, and support both a 30-day lunar surface mission and a 1,200-day Mars-forward mission with maintainable modular hardware.

2.2 Solution Overview

PHAT integrates a thermoelectric cold-water subsystem into the ISS PWD heritage architecture while preserving independent hot and ambient dispensing. The system operates in four modes: hot, ambient, cold, and flush. In hot and ambient modes, water follows the heritage PWD flow path. In cold mode, iodinated potable water is routed through a single-pass 316L stainless-steel serpentine pipe cooled by ten externally mounted thermoelectric cooler (TEC) stages. Each TEC cold face couples to the pipe through a machined copper saddle block; copper remains external to the wetted flow path. The TEC hot side rejects heat to a liquid heat-exchanger block connected to the spacecraft coolant loop, and the cold-side assembly is enclosed in aerogel insulation for condensation control.

The cold branch uses a flow-through architecture rather than a stagnant reservoir or dead-leg cooling volume. This preserves the ISS PWD design philosophy, limits microbial-growth risk, and allows the cold-water function to be developed, tested, and replaced as a discrete subsystem.

ACTEX remains the iodine-removal element in the water path, while an in-line UV-C module provides microbial-control redundancy. The UV-C module does not replace ACTEX because iodine removal is a chemical function, but it reduces the risk of single-point microbial-control failure on long-duration missions. The module would also decrease the hours spent on replacement of filters as traditionally, 0.2-micron filters were used to catch microbes. This is more efficient for short duration missions as the filter needed to be replaced every 6 months. In addition, the crew would spend hours replacing the micron filters and is an orbital replacement unit. Thus, UV-C filter would be advantageous for a cislunar and/or interplanetary mission which has an increased shelf life and would lessen the hours spent on replacement.[16]

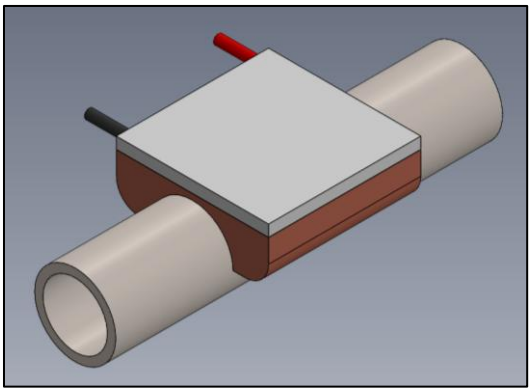

Figure 2-1. PHAT cold-loop hardware concept

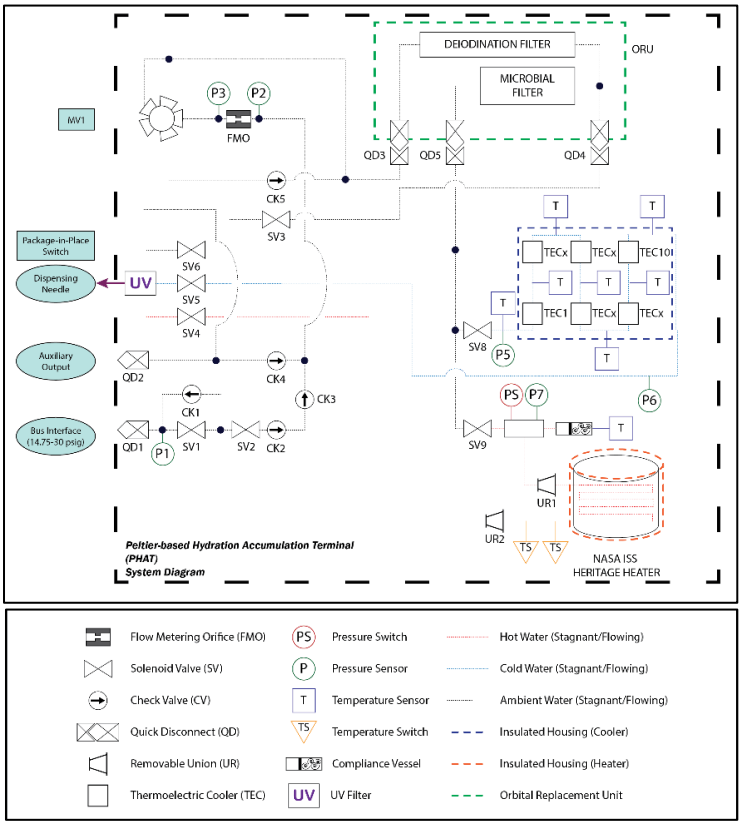

Figure 2-2. PHAT system architecture diagram

Table 2-1: Baseline PHAT Architecture Parameters

Parameter	Baseline PHAT value	Rationale
Dispense modes	Hot, ambient, cold, flush	Preserves ISS PWD function and adds cold-water capability
Cold-water target	≤16°C outlet	Meets NASA-STD-3001 cold potable-water range
Process flow rate	0.50 L/min	Dispenses 250 mL in approximately 30 s
Cold loop	1.5 m, 3/4 in. Schedule 10 316L stainless pipe	Iodinated-water compatibility [3]; single-pass flow avoids dead legs
TEC array	10 × 180 W-class modules	Meets 27°C cabin worst case within power budget
Hot-side rejection	Liquid heat exchanger, $R_{sink} \approx 0.042$ K/W	Air-cooled sink was infeasible at worst case
Worst-case TEC power	421 W at 27°C cabin	Below 2 kW payload power allocation
Worst-case heat rejection	~0.8 kW to coolant loop	Process-water heat plus TEC electrical input
Microbial control	ACTEX + UV-C	ACTEX removes iodine; UV-C adds disinfection redundancy
Condensation control	60 mm aerogel enclosure	Keeps outer surface above worst-case dew point

2.3 Design Constraints and Compliance

Table 2-2 summarizes PHAT compliance with the HuLC design constraints. The design approach is to preserve the TRL-9 ISS PWD core and isolate new development risk within a modular cold-water subsystem.

Table 2-2. PHAT compliance with HuLC design constraints.

Constraint	PHAT compliance approach	Remaining verification
Minimal barriers to NASA adoption	Heritage-first architecture; cold function isolated from hot and ambient dispensing. Fits within two Express Rack lockers; worst-case TEC draw is 421 W with budget of 2000W [14]. Mass, size, and cost are quantified in Sections 5 and 7.	CAD packaging, interface-control document, and mass-reduction trade during breadboard design.
No additional crew risk	No refrigerants, compressors, flammable working fluids, or added pressurized gases. A TEC-branch failure causes loss of cold water only; hot and ambient paths remain available. All external interfaces are sealed against lunar dust ingress expected during EVA suit doffing and airlock cycling; 316L stainless steel surfaces minimize dust adhesion per SLS-SPEC-159 Section 3.4.2.2.3 [4].	Fault detection and isolation, electrical safety, radiation-tolerant electronics, and crew-procedure validation.
Launch-load survivability	Rack-mounted packaging, short-supported fluid runs, compact TEC blocks, and a 316L stainless flow path provide a structurally robust concept without fragile wetted heat exchangers.	Static-load, random-vibration, workmanship, and leak testing per the DT&E plan.
30-day lunar mission life	No cold-loop consumables limit a 30-day mission. At eight uses per day, the lunar mission imposes about 240 TEC thermal cycles.	HLS interface verification and crew-use validation in a representative cabin environment.
1,200-day Mars-forward life	At eight uses per day, the Mars-forward case imposes about 9,600 TEC cycles. The architecture includes ACTEX replacement logistics, UV-C redundancy, hot-side fouling margin, and modular TEC replacement.	Long-duration coolant-loop, microbial-control, UV-C lifetime, and spare-module validation.
Targeted use within 5–8 years	Flight readiness by 2033 is enabled by ISS PWD heritage, mature TEC components, and phased maturation of only the cold-loop subsystem.	TRL 5 component tests, TRL 6 integrated breadboard, TRL 7 ISS demonstration, and TRL 8 HLS certification.

Major changes since the Phase 1 proposal are summarized in Table 2-3. These updates respond to reviewer feedback and to Phase 2 thermal and materials analysis.

Table 2-3. Changes since the proposal phase.

Driver	Design change	Reason
Avoid stagnant water and dead legs	Changed cold branch to a single-pass flow-through pipe	Reduces microbial-growth risk and follows ISS PWD practice
Improve dispense-volume accuracy	Added flow-meter-based volume measurement	Addresses judge concern about orifice-only delivery uncertainty
Insulate sub-dew-point hardware	Added sealed aerogel cold-side enclosure [9]	Prevents condensation and parasitic heat gain
Improve hot-side feasibility	Replaced air-cooled heat sinks with liquid heat-exchanger blocks	Reduces hot-side thermal resistance and enables worst-case operation
Maintain material compatibility	Replaced copper wetted block with 316L pipe plus external copper saddle	Keeps copper out of iodinated potable water
Increase thermal margin	Changed from a 6-module concept to a 10-module sequential TEC array	Meets the ≤16°C outlet target at 27°C cabin
Strengthen implementation basis	Added subsystem TRL assessment, V&V plan, and revised cost model	Aligns the paper with Phase 2 scoring criteria

2.4 Innovation and Design Rationale

PHAT's innovation is not a new water dispenser from scratch; it is a low-risk extension of a proven spacecraft water-dispenser architecture. The design combines heritage fluid handling with a solid-state, modular cold-water branch sized by original thermal analysis. This approach differentiates PHAT from terrestrial water chillers and unreliable vapor-compression systems [8] by avoiding refrigerants, gravity-dependent components, and compressor wear while preserving flight-proven PWD functions.

2.5 Engineering Analysis Summary

The PHAT cold-loop sizing is based on a sequential thermoelectric model documented in Appendix A. Each of the ten TEC stages is solved using its local inlet water temperature, cold-side resistance through the stainless pipe and copper saddle, and hot-side resistance to the liquid coolant loop. This stage-by-stage approach captures the declining cooling capacity and COP of downstream modules as the water temperature approaches the 16°C outlet target. A lumped single-temperature model would miss this downstream performance roll-off and understate the required thermal margin.

Table 2-4. PHAT cold-water performance summary — ten TEC modules, liquid heat-exchanger hot side, 0.50 L/min process flow.

Cabin ambient (°C)	Outlet temp. (°C)	Current/module (A)	TEC power (W)	Cooling removed (W)	System COP
18.0	15.90	1.15	11	73.0	6.87
22.5	15.94	3.92	122	228.2	1.88
27.0	16.00	7.36	421	382.6	0.91

The 16°C target is the NASA-STD-3001 cold water upper bound [2], the maximum temperature that qualifies as cold, not a dispensing preference. At the 27°C worst case this requires 7.36 A per module and is the binding design point. At the more typical 18°C and 22.5°C cabin conditions, the array reaches 16°C at only 1.15 A and 3.92 A, leaving headroom for the PID to drive the outlet meaningfully lower toward crew-preferred drinking temperatures.

The steady-state model meets the ≤16°C outlet target for all evaluated HLS cabin conditions. At the 27°C worst case, the cold loop removes 382.6 W from the water, consumes 421 W of electrical power, and rejects approximately 803.6 W to the spacecraft coolant loop. The 7.36 A/module operating point remains below the 15 A module limit, leaving current headroom for degraded heat rejection, elevated cabin temperature, or controller margin. Table 2-5 provides the per-module breakdown at worst case, illustrating the progressive cooling behavior that motivates the sequential model.

Table 2-5. Per-module breakdown at worst case (T_amb = 27°C, I = 7.36 A/module). T_cf = TEC cold-face temperature.

Module	T_{in} (°C)	T_{out} (°C)	q_{cold} (W)	P_{elec} (W)	COP	T_{cf} (°C)	Notes
1	27.00	25.73	44.24	41.19	1.07	6.6	Warmest inlet; highest COP
2	25.73	24.50	42.79	41.41	1.03	6.0	
3	24.50	23.31	41.39	41.62	0.99	5.4	
4	23.31	22.16	40.04	41.83	0.96	4.8	
5	22.16	21.04	38.73	42.03	0.92	4.3	
6	21.04	19.97	37.46	42.23	0.89	3.8	
7	19.97	18.92	36.23	42.41	0.85	3.3	
8	18.92	17.92	35.05	42.60	0.82	2.8	
9	17.92	16.94	33.90	42.77	0.79	2.3	
10	16.94	16.00	32.79	42.94	0.76	1.8	Coldest outlet; min COP
Total	**27.00**	**16.00**	**382.6**	**421.0**	**0.91**	-	

Table 2-6. Engineering analysis conclusions retained in the report body.

Engineering issue	Body-level conclusion	Detailed support
Hot-side cooling	Air cooling was infeasible at worst case; the liquid heat exchanger enables 421 W operation and ~0.8 kW heat rejection.	Appendix A hot-side cooling trade
Condensation and freezing	The final TEC cold face remains above freezing at 1.8°C; 60 mm aerogel keeps the outer surface above the 22°C worst-case dew point.	Appendix A insulation sizing
Heater compatibility	The heritage ISS PWD heater remains on an independent hot-water path; hot and cold branches do not share the same thermal conditioning path.	Appendix A heater estimate
Gravity compatibility	Pressure-fed PWD flow, TEC operation, and forced-convection coolant flow are not gravity-dependent.	Section 3 V&V and TRL plan
Long-duration fouling	A 25–50% hot-side resistance increase still meets the 16°C target within the power budget, increasing worst-case TEC power from 421 W to 446–474 W.	Appendix A fouling sensitivity
Power interface	Cold-loop operation uses 421 W worst case against the 2 kW payload allocation; the heater operates on an independent path.	Sections 5 and 7 assumptions

2.6 Operational Feasibility, Maintainability, and Scaling

PHAT preserves the ISS PWD crew-interface philosophy while adding a cold-water selection mode. Hot mode remains limited by the heritage heater recovery cycle between consecutive hot dispenses [1]. Cold mode operates differently: the TEC array conditions the cold branch, and dispense time is set primarily by process flow rate. At 0.50 L/min, fill times range from approximately 3 s for 25 mL to 30 s for 250 mL. The retained downstream volume of approximately 123.8 mL is purged over about 11–21 s before cold water reaches the nozzle after standby; consecutive cold dispenses require only this purge interval. The interface retains one-handed operation with drink bags and food pouches, adding cold mode without changing the basic crew interaction model.

For a 30-day lunar mission, PHAT imposes no limiting cold-loop consumables and accumulates approximately 240 TEC thermal cycles at eight uses per day. For a 1,200-day Mars-forward

mission, scheduled maintenance consists of ACTEX replacement (estimated 7 replacements at 15–20 min each, assuming a 6-month interval), coolant-loop filter cleaning (estimated 7 events at 30 min each), and weekly system flushes of approximately 5 min each. Estimated total crew maintenance time is on the order of 120–130 hours over the mission, or roughly 6 min/day — consistent with NASA's goals for sustainable autonomous operations [5] [6].

The ten-module cold loop is sized for 0.50 L/min and the 27°C HLS cabin worst case. Higher-throughput Mars applications can scale by adding TEC stages, using parallel cold loops, or adjusting process flow rate. The same sequential model applies to scaled configurations; verification should confirm coolant temperature and flow, 28 VDC TEC drivers, ACTEX interval, UV-C lifetime, and launch-stable insulation.

3 Verification and Validation

3.1 Testing Approach

Prior to building the full prototype, two off-the-shelf 180 W aquarium Peltier modules were tested individually in a flow-through configuration to characterize baseline cooling performance. Modules were connected in series with plastic tubing, with copper water blocks on the cold face of each module and air-cooled finned heat sinks with fans on the hot side. Inlet and outlet water temperatures were measured with thermocouples, flow speed was measured volumetrically, and total electrical power draw was recorded.

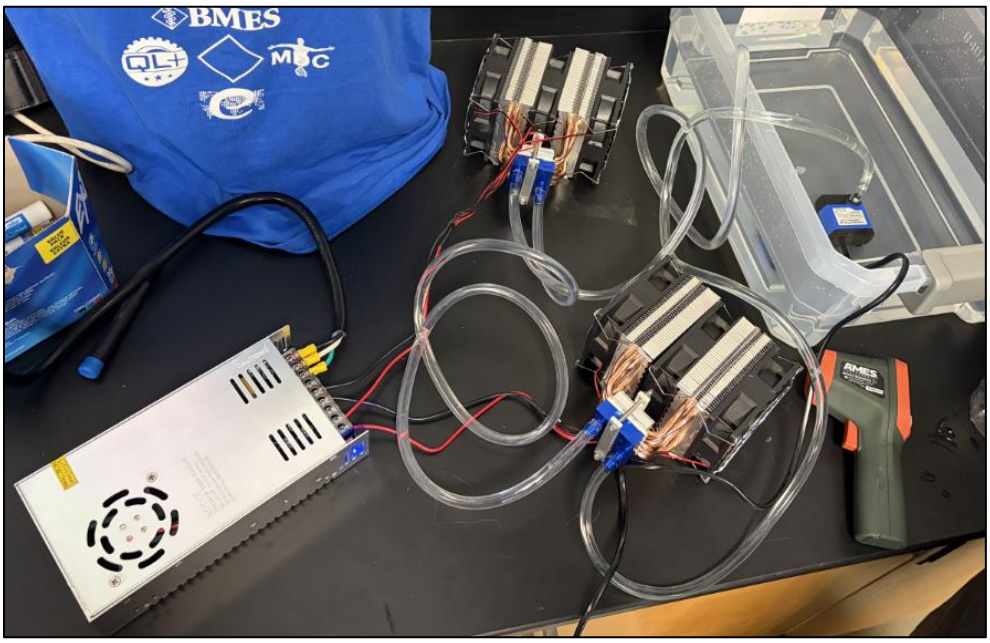

Figure 3-1. Bench test setup showing two aquarium Peltier modules with copper water blocks, plastic tubing, and fan-cooled heat sinks.

Table 3-1 summarizes the bench test results alongside the analytically optimized ten-module configuration from Section 2.6.

Table 3-1. Bench test results vs. analytically optimized PHAT configuration.

Condition	Inlet (°C)	Outlet (°C)	ΔT (°C)	Power (W)	Flow Speed (m/s)
Bench test (2 modules, fan-cooled)	25	23	2	360.0	0.83
Optimized model (10 modules, liquid-cooled)	27	16	11	421.0	0.021

The bench test confirmed that Peltier modules can be integrated into a flow-through water loop and that the sequential resistance-network model in Appendix A correctly identifies the dominant loss mechanisms. The analytical model subsequently evolved into the finalized 10-module stainless-steel serpentine architecture documented in Appendix A.

3.2 Cal Poly Senior Project Prototype

A functional prototype was independently developed as part of a Cal Poly Mechanical Engineering senior project, predating the HuLC competition. While not built as a competition deliverable, it provided valuable hands-on experience with TEC behavior and flow-path routing that directly informed the PHAT design. The prototype demonstrates three dispensing modes (hot, ambient, and cold) using solenoid valves controlled by a PLC and Arduino, with two TEC stages on the cold path.

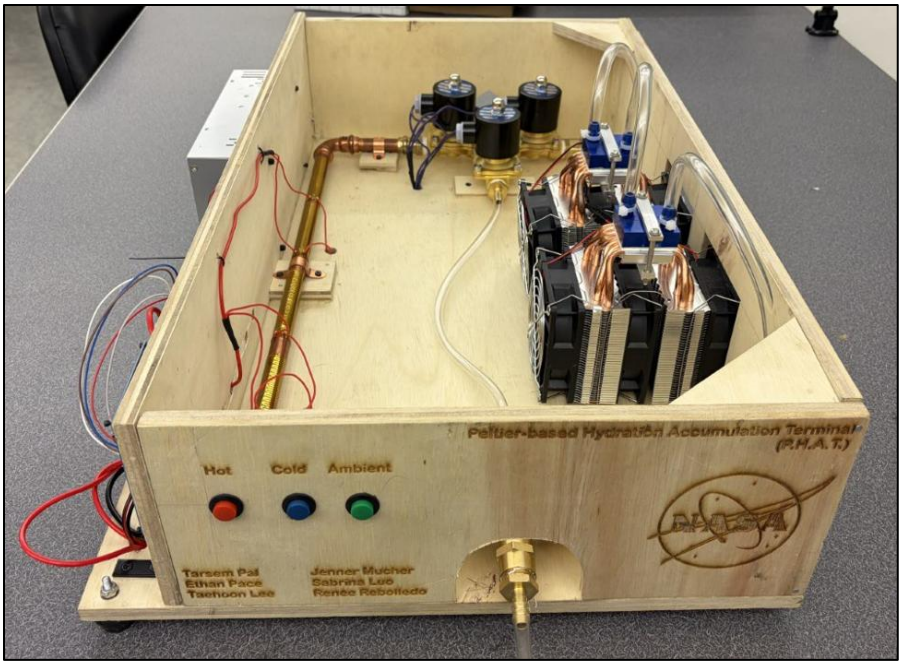

Figure 3-2. Cal Poly senior project prototype showing wood chassis, copper and plastic tubing, solenoid valves, and three-mode dispensing interface.

3.3 Obstacles and Mitigations

3.3.1 Insufficient residence time

The bench test flow speed of 0.83 m/s gave water inadequate contact time with the cold block surface to absorb meaningful cooling. The optimized design reduces flow speed to 0.066 m/s (a 40× reduction) increasing residence time sufficiently for each of the ten modules to contribute to a progressive temperature drop, as modeled in Table x.

3.3.2 Inadequate hot-side heat rejection

Air-cooled heat sinks with fans produced a high hot-side thermal resistance, saturating the hot junction temperature and severely degrading module COP. As detailed in Section 2.2, thermal modeling showed that an air-cooled hot side is infeasible for a multi-module configuration at worst-case cabin conditions. The optimized design replaces fan cooling with a liquid heat exchanger ($R_{sink} \approx 0.042$ K/W), keeping the hot junction near 31°C and making the ten-module configuration feasible within the available power budget.

3.3.3 Uninsulated lines

Uninsulated connecting runs allowed heat pickup from the ambient environment between modules. The optimized design encloses the entire cold loop within a 60 mm aerogel insulation jacket ($k \approx 0.024$ W/m·K) to prevent both heat pickup and condensation on sub-dewpoint surfaces. Together these changes account for the substantial gap between bench and model performance.

4 Realistic Technology Assumptions

Table 4-1 summarizes the current Technology Readiness Level (TRL) of each PHAT subsystem using NASA's standard TRL definitions [7]. The ISS PWD heritage core enters the program at TRL 9, eliminating re-qualification risk for hot and ambient dispensing. The TEC modules carry TRL 6 flight heritage from spacecraft instrument cooling [11]. All new development risk is isolated to the thermoelectric cold-loop hardware and the integrated system, both currently at TRL 3.

Table 4-1. PHAT Subsystem Technology Readiness Levels [7].

Subsystem	TRL	Basis per [7]
ISS PWD Heritage Core (heater, valves, filters)	9	Actual system flight proven through successful mission operations [1] [15]
TEC modules	6	Component prototype demonstrated in operational environment [11]
Stainless-steel serpentine pipe / copper saddle / liquid heat-exchanger	3	Analytical model developed and validated against datasheet predictions (Appendix A); no breadboard hardware built
Aerogel condensation enclosure	3	Analytical proof of concept complete (Section 2.6.2); no hardware fabrication
Integrated PHAT system	3	System-level design and analysis complete; no integrated hardware

5 Mass and Size Estimates

5.1 Envelope

PHAT is designed to fit within a double Express Rack locker, providing a usable envelope of approximately 906 mm wide × 1,274 mm high × 500 mm deep.

5.2 Mass

A detailed mass budget requires a CAD and hardware procurement, both planned for the 2026-2027 component testing phase. Below, Table 5-1 provides a bottom-up estimate based on component datasheets and catalog values, anchored against the ISS PWD heritage mass of approximately 16 kg [1] as a reference.

Component	**Basis**	**Estimated Mass (kg)**
ISS PWD heritage core (heater, valves, filters, structure)	*Placeholder for cost estimation; not confirmed in published sources [1]*	16.0
10× TEC modules (180 W class)	Datasheet (TEC1-12715, 50 g each)	0.5
3/4" Sch. 10 316L SS serpentine pipe, est. 1.5 m	Catalog: 1.63 kg/m	0.9
10× copper saddle blocks	CAD estimate, 200 g each (SolidWorks)	2.0
10× liquid heat-exchanger blocks	Engineering estimate, 300 g each	3.0
Aerogel insulation enclosure	Bulk density ≈ 5 kg/m³, est. 0.008 m³	0.5
Solenoid valves, check valves, fittings (14 items)	Catalog: ≈ 200 g each	2.8
Electronics, wiring, PLC	Engineering estimate	2.0
Structure, mounting, miscellaneous	15% margin on cold-loop subtotal	2.3
Cold-loop subsystem subtotal	Items 2-9 above	14.0
Heritage core (placeholder)	**Pending verification**	**16.0**
Total P.H.A.T. (placeholder)	**Pending verification**	**30.0**

Table 5-1. PHAT system mass estimate. Heritage core is a placeholder (16 kg) for cost estimation pending source verification. Cold-loop items carry ±20–30% uncertainty; 15% margin applied to subtotal.

The cold-loop addition is estimated at approximately 13.5 kg. A mass reduction trade focused on the heat-exchanger blocks and structural elements is recommended during detailed design.

6 Proposed Path-to-Flight Project Timeline

PHAT's development strategy leverages the TRL-9 ISS PWD heritage core to isolate risk to the thermoelectric cooling subsystem, targeting flight readiness by 2033 for infusion into an Artemis HLS mission. **Table 6-1** outlines the phased DT&E schedule; all new development risk is contained within the thermoelectric cooling subsystem and the heritage dispensing core requires no re-qualification. TRL levels follow NASA definitions per [7].

Year	Phase	Key Activities	TRL Exit
2026-2027	Component Testing	Single-module TEC breadboard; aerogel condensation chamber test; UV-C compatibility and ACTEX replacement interval testing	5
2028-2029	Subsystem Integration	Ten-module array validation; closed-loop controller demonstration; integrated PHAT breadboard; launch load testing per GSFC-STD-7000	6
2030-2032	Flight Demonstration	180-day ISS Express Rack demonstration validating cold dispensing in microgravity and TEC thermal cycle accumulation	7
2033	HLS Certification	HLS integration; human factors testing with gloved hands in partial gravity; flight certification per SLS four-phase framework [12]	8
2033+	Flight Operations	Artemis lunar surface mission	9

Table 6-1. PHAT Path-to-Flight Schedule

6.1 Scaling

The ten-module array is sized for 0.50 L/min and the 27°C HLS cabin worst case. For Mars transit with a larger crew or higher throughput requirement, additional TEC stages or parallel cold loops can be added without modifying the heritage dispensing core. The sequential resistance-network model in Appendix A applies directly to any scaled configuration, and aerogel enclosure thickness can be recalculated for any ambient temperature and humidity envelope using the same steady-state conduction-convection balance.

7 Budget Assessment

To assess the budget and cost of the PHAT system’s design and implementation, NASA’s own Project Cost Estimating Capability (PCEC) version 2.4 add-in for Microsoft Excel was used. Modeling the PHAT as a crew system with a multi-variable CER, the add-in was able to calculate a reasonable budget estimation. In order to arrive at a value, the system was assumed to be used once each in two missions, the first being to the Moon and the second to Mars, with a total period of 10 years between the beginning of development to the second mission. Production was expected to mature at a normal unit rate according to the Crawford theory of learning and the system test hardware cost was set at 130% the cost of a flight unit, which is historically the standard approximation. Additionally, to compare to the historical development of the ISS PWD, the analogous adjustment factors of the ISS Water Recovery System were used to develop the CER.

Using an approximate mass of 35 pounds for the ISS PWD and the approximate 74 pound mass of the PHAT, the budget approximation was formulated, seen below in Table 7-1.

Table 7-1. Budget estimation of PHAT compared to ISS PWD, in millions of dollars.

	PHAT	**ISS PWD**
Cost Allocation	[$M]	[$M]
Design & Development Cost	$ 4.89	$ 2.38
System Test Hardware Cost	$ 1.70	$ 0.72
Flight Unit Cost	$ 1.31	$ 0.55
Total Production Cost	$ 2.62	$ 1.11
Average Cost per Unit	$ 1.31	$ 0.55
Total Cost	$ 9.21	$ 4.20

The ISS PWD cost was calculated the same as the PHAT cost, however by using the smaller assumed mass of the ISS PWD. However, this cost estimate will be higher than would actually be expected should the same exact design be reused and is merely a ballpark figure to show an alternative solution where the PWD is redesigned and tested from scratch for the future human lander missions. By modeling both, we can see that the cost of designing a novel system instead of using an adapted version of the ISS PWD increases the cost by a factor of 2.2, which is no small amount. In the grand scheme of the mission cost, it is but a drop in the pond, but it would be up to the decision-making bodies at NASA to decide whether or not cold water is worth the price.

8 Full Concept / Mission Architecture Timeline

PHAT is designed as a modular potable-water thermal-conditioning upgrade for two mission classes: a 30-day Artemis/HLS lunar surface mission and a 1,200 Mars-forward transit and surface mission. This section maps the development path from Section 6 into operational mission architecture, showing how the same core hardware transitions from subsystem validation to lunar deployment and Mars-forward scaling. TRL levels follow NASA definition per [7].

Timeframe	PHAT Milestones	TRL	Lunar Relevance	Mars Relevance
2026-2027	Component-level TEC breadboard; pipe/saddle thermal validation; aerogel and UV-C testing	5	Retires primary cold-loop risks before HLS integration	Establishes baseline thermal and materials data for long-duration scaling
2028-2029	Integrated ten-module breadboard; outlet-temperature and freeze protection control; launch-load testing	6	Demonstrates cold-water subsystem survives launch and operates as HLS cabin subsystem	Validates modular architecture for expanded crew sizes or parallel cold loops
2030-2032	180-day microgravity demonstration on ISS Express Rack	7	Validates cold dispensing, condensation control, and crew interface in microgravity	Provides long-duration TEC cycling, coolant-loop stability, and microbial control data
2033	HLS integration, human factors evaluation, and flight certification	8	Certifies PHAT for HLS crew-cabin water dispensing	Produces interface data applicable to Mars transit habitat water systems
2033+	First operational lunar surface deployment	9	30-day lunar mission with hot, ambient, and cold dispensing	Validates operational procedure before Mars-forward adoption
Post-lunar	Scaled integration into Mars transit or surface habitat	8-9	Lunar flight data informs design updates and maintenance intervals	Supports 1,200 day operation with modular TEC replacement and scheduled consumable logistics

Table 8-1. PHAT full concept and mission architecture timeline

Lunar Mission

PHAT operates as a drop-in upgrade to the HLS crew-cabin water system, preserving heritage hot and ambient dispensing while adding cold water delivery. The 30-day mission imposes approximately 240 TEC thermal cycles, well within the qualified module life [13].

Mars-forward Mission

The modular ten-module architecture scales by adjusting module count, flow rate, or parallel cold loops depending on crew size and cabin thermal conditions. The sequential resistance-network model in Appendix A applies directly to any scaled configuration. Long-duration operation requires a logistics plan for ACTEX filter replacement, UV-C module lifetime tracking, and spare TEC availability – all supported by the maintenance architecture described in Section 2.7.

9 Conclusions and Key Findings

PHAT closes a direct gap in NASA's crew life support capability (no current spaceflight potable water dispenser meets the NASA-STD-3001 cold water requirement [2]) by adding solid-state thermoelectric cooling to the flight-proven ISS PWD heritage design. The heritage-first architecture minimizes development and programmatic risk by isolating all new functionality within a modular, crew-replaceable cold-loop subsystem that cannot compromise existing hot and ambient dispensing. Thermal analysis confirms the ten-module configuration meets the 16°C outlet target across all HLS cabin conditions within the available power budget. The system installs within two standard Express Rack lockers, requires no new spacecraft interfaces, and has a clear scaling path to Mars transit configurations. A phased DT&E path targets TRL 8 flight certification by 2033, leveraging ISS for microgravity demonstration before integration into the HLS crew cabin.

Further research should be conducted on the thermoelectric coolers to decrease the number of coolers needed for the water dispenser. This would limit production and design cost, as well as the mass budget. The initial findings for cost suggest that PHAT would be twice as expensive compared to the current PWD design by integrating a cold-water system. In terms of going with the modulus, NASA would have to decide whether implementing a cold section with Peltier coolers would be worth the cost.

Citations

[1] L. Shaw and J. Barreda, “International Space Station USOS Potable Water Dispenser Development.”
NASA Lyndon B. Johnson Space Center, [Online], 2008, Available: https://ntrs.nasa.gov/api/citations/20080013432/downloads/20080013432.pdf

[2] National Aeronautics and Space Administration (NASA), “NASA-STD-3001, Volume 2: Human Factors, Habitability and Environmental Health,” Revision D, Office of the Chief Health and Medical Officer, [Online], 2023, Available: https://www.nasa.gov/ochmo/human-spaceflight-and-aviation-standards/

[3] Mudgett, P., Flanagan, D., Schultz, J., and Sauer, R., “Depletion of Biocidal Iodine in a Stainless Steel Water System,” SAE Technical Paper 941391, 1994, Available: https://doi.org/10.4271/941391.

[4] Frank B. Leahy, “SLS-SPEC-159, ROSS-PROGRAM DESIGN SPECIFICATION FOR NATURAL ENVIRONMENTS (DSNE),” Revision I [Online], 2021, Available: https://ntrs.nasa.gov/api/citations/20210024522/downloads/SLS-SPEC-159%20Cross-Program%20Design%20Specification%20for%20Natural%20Environments%20(DSNE)%20REVISION%20I.pdf

[5] National Aeronautics and Space Administration (NASA), “NASA’s Plan for Sustained Lunar Exploration and Development,” [Online], Available: https://www.nasa.gov/wp-content/uploads/2020/08/a_sustained_lunar_presence_nspc_report4220final.pdf?emrc=5aa8ef

[6] Lisa Watson-Morgan, et. al., “NASA’s Initial and Sustained Artemis Human Landing Systems,” [Online], Available: https://ntrs.nasa.gov/api/citations/20205008849/downloads/final%20HLS%20IEEE%20paper.pdf

[7] National Aeronautics and Space Administration (NASA), "Technology Readiness Level Definitions," [Online]. Available: https://www.nasa.gov/wpcontent/uploads/2017/12/458490main_trl_definitions.pdf

[8] Z. Huang and T. Li, “Experimental Investigation of Gravity Effect on a Vapor Compression Heat Pump System,” *Energies*, vol. 16, no. 11, p. 4412, 2023. [Online]. Available: https://www.mdpi.com/1996-1073/16/11/4412

[9] NASA, “Aerogels: Thinner, Lighter, Stronger - NASA,” *NASA*, Jul. 28, 2011. Available: https://www.nasa.gov/aeronautics/aerogels-thinner-lighter-stronger/

[10] Maryatt, B. W. (2019). Lessons learned for the International Space Station potable water dispenser. NASA Johnson Space Center. https://ttu-ir.tdl.org/server/api/core/bitstreams/028fd2b1-34ca-4dac-be77-7457a31470a0/content

[11] “7.0 Thermal Control - NASA,” *NASA*, Oct. 16, 2021. Available: [Online] https://www.nasa.gov/smallsat-institute/sst-soa/thermal-control/#7.3.3

[12] J. Kress, W. Bordelon, Jr., L. Beech, and D. Diecidue-Conners, “Flight Certification Approach for NASA’s Space Launch System,” *NASA Marshall Space Flight Center*, [Online], Aug. 6, 2024, Available: https://ntrs.nasa.gov/citations/20240007646

[13] TEC Microsystems GmbH, “Thermoelectric Coolers Reliability Testing and Reports,” [Online]. Available: https://www.tec-microsystems.com/faq/reliability-testing-and-reports.html.

[14] R. E. Lake, "Conducting Research on the ISS using the EXPRESS Rack," NASA Marshall Space Flight Center, NTRS 20140016876. Available: https://ntrs.nasa.gov/search.jsp?R=20140016876

[15] Toon, K. P., & Lovell, R. W. (2010). International Space Station USOS Potable Water Dispenser on-orbit functionality vs. design. NASA Lyndon B. Johnson Space Center. https://ntrs.nasa.gov/api/citations/20100014345/downloads/20100014345.pdf

[16] NASA, “Deep Space Hydration,” *Houston We Have a Podcast*, Episode 293, NASA Johnson Space Center, May 12, 2023. [Online]. Available: https://ntrs.nasa.gov/api/citations/20100014345/downloads/20100014345.pdf

Appendices

Appendix A: P.H.A.T. Peltier Cooler — Sequential Thermal Model

Appendix B: Cost Estimate

P.H.A.T. Peltier Cooler — Sequential Thermal Model

Design Study Report and Appendix

Attachment A to HuLC 2026 Technical Paper

Tarsem Pal Cal Poly SLO ME Senior Project Team

May 28, 2026

Contents

1 System Overview

This appendix documents the sequential thermal model used to size the P.H.A.T. cold-water subsystem. Iodinated water flows single-pass through a ¾" Schedule 10 316L stainless steel serpentine pipe at 0.50 L/min. Ten 180 W-class TEC modules are clamped to the exterior of the pipe via machined copper saddle blocks, which conform to the pipe curvature and reduce contact resistance. A liquid heat-exchanger block on the TEC hot side rejects waste heat to a coolant loop. The entire cold-side assembly is sealed within an aerogel-insulated enclosure. The objective is to deliver outlet water at $\leq 16\,^{\circ}\mathrm{C}$ across cabin ambient temperatures of $18\,^{\circ}\mathrm{C}$ to $27\,^{\circ}\mathrm{C}$.

1.1 Thermal Path and Material Rationale

The cold-side thermal path at each module (direction of heat flow, not temperature ordering) is:

$$T_{\text{water}} \xrightarrow{R_{\text{conv}}} T_{\text{pipe,ID}} \xrightarrow{R_{\text{pipe}}} T_{\text{pipe,OD}} \xrightarrow{R_{\text{contact}}} T_2 \xrightarrow{\text{TEC}} T_1 \xrightarrow{R_{\text{sink}}} T_{\text{coolant}} \tag{1}$$

Process water contacts *only* the 316L stainless steel pipe interior. The copper saddle block sits on the pipe exterior and is not a wetted component. This is critical: the water contains dissolved iodine biocide (6.0 mg/L before ACTEX filtration), which is incompatible with copper. The stainless steel pipe provides the iodine-compatible wetted surface; the copper saddle provides efficient thermal coupling between the pipe OD and the flat TEC cold face.

Stainless steel is selected as the wetted material for compatibility relative to copper, but it is not chemically inert in iodinated water. Mudgett et al. [4] demonstrated measurable depletion of biocidal iodine in stainless steel spacecraft water-system tubing, particularly under stagnant high surface-area-to-volume conditions. The design therefore retains operational mitigations including periodic flush procedures after extended inactivity and continued material compatibility validation testing.

1.2 Hot-Side Cooling Selection

Hot-side cooling selection was based on a thermal feasibility analysis across both air-cooled and liquid-cooled configurations. An air-cooled finned heat sink ($R_{\text{sink}} \approx 0.175\,\mathrm{K/W}$) requires more than ten modules drawing over 1700 W to meet the $27\,^{\circ}\mathrm{C}$ worst case, exceeding the payload power budget. A liquid heat exchanger ($R_{\text{sink}} = 0.042\,\mathrm{K/W}$) keeps the hot junction near $31\,^{\circ}\mathrm{C}$ and achieves the ten-module target at 421 W — well within the 2000 W allocation. Liquid hot-side cooling is therefore the baseline.

1.3 Sequential Model

The pipe is divided into $M = 10$ segments, one per TEC module. Water cools stage by stage:

$$T_{out,k} = T_{in,k} - \frac{q_{cold,k}}{\dot{m}\, c_{p,w}}, \qquad T_{in,k+1} = T_{out,k} \tag{2}$$

Downstream modules receive colder water, operate against a larger junction ΔT, pump *less* heat, draw *more* electrical power, and exhibit *lower* module-level COP. A lumped model that assigns a single bulk temperature to all modules would miss this stage-to-stage variation entirely.

2 TEC Module — Bergman Section 3.7.2

2.1 Governing Equations

The heat rates at the hot (T_1) and cold (T_2) faces during cooling operation are (Bergman, Sec. 3.7.2 [1]):

$$\boxed{q_{\text{cold}} = I\, S_{p\text{-}n}\, T_2 - \frac{I^2 R_e}{2} - \frac{T_1 - T_2}{R_t}} \tag{3}$$

$$\boxed{q_{\text{hot}} = I\, S_{p\text{-}n}\, T_1 + \frac{I^2 R_e}{2} - \frac{T_1 - T_2}{R_t}} \tag{4}$$

$$P_{\text{elec}} = q_{\text{hot}} - q_{\text{cold}} = I\, S_{p\text{-}n}(T_1 - T_2) + I^2 R_e \tag{5}$$

The three terms represent Peltier pumping, Joule self-heating (split equally to each face), and Fourier back-conduction. Temperatures in the Seebeck terms are absolute (K).

Face temperatures couple to the external network:

$$T_1 = T_{\text{coolant}} + q_{\text{hot}}\, R_{\text{sink}}, \qquad T_2 = T_{\text{water}} - q_{\text{cold}}\, R_{\text{cold}} \tag{6}$$

solved iteratively with adaptive under-relaxation until $|T^{(n+1)} - T^{(n)}| < 10^{-6}$.

2.2 Parameter Back-Calculation

Effective module properties are back-calculated from four datasheet values at the rated hot-side temperature $T_h = 299.8\,\text{K}$ (80):

$$\text{Eq 1 (max cooling, } \Delta T = 0\text{):} \quad Q_{\max} = S\, I_{\max}\, T_h - \tfrac{1}{2} I_{\max}^2 R_e \tag{7}$$

$$\text{Eq 2 (max } \Delta T\text{, } q_c = 0\text{):} \quad 0 = S\, I_{\max}\, T_c - \tfrac{1}{2} I_{\max}^2 R_e - \frac{\Delta T_{\max}}{R_t}, \quad T_c = T_h - \Delta T_{\max} \tag{8}$$

$$\text{Eq 3 (terminal voltage):} \quad V_{\max} = S\, \Delta T_{\max} + I_{\max}\, R_e \tag{9}$$

Voltage relation. Equation 3 uses the junction *temperature difference* $\Delta T_{\max}$, since the Seebeck back-EMF at the rated condition opposes the drive voltage in proportion to the junction ΔT. Substituting the absolute hot-side temperature T_h in its place is a common error that inflates the Seebeck term and drives $R_e \to 0$, suppressing Joule heating; the form above avoids this and yields a physical electrical resistance.

Solving Eqs 1 and 3 simultaneously:

$$S = \frac{Q_{\max} + \tfrac{1}{2} I_{\max} V_{\max}}{I_{\max}\big(T_h + \tfrac{1}{2}\Delta T_{\max}\big)}, \qquad R_e = \frac{V_{\max} - S\, \Delta T_{\max}}{I_{\max}} \tag{10}$$

then from Eq 2:

$$R_t = \frac{\Delta T_{\max}}{S\, I_{\max}\, T_c - \tfrac{1}{2} I_{\max}^2 R_e} \tag{11}$$

3 System Parameters

Table 1: Pipe geometry — 3/4" Schedule 10 316L stainless steel.

Parameter	Symbol	Value
Outer diameter	D_o	26.67 mm (1.050")
Wall thickness	t_w	2.11 mm (0.083")
Inner diameter	D_i	22.45 mm (0.884")
Pipe conductivity (316L)	k_p	16.3 W/(m · K)

Table 2: Water properties at 20 °C.

Parameter	Symbol	Value
Density	ρ_w	998 kg/m^3
Specific heat	$c_{p,w}$	4182 J/(kg · K)
Conductivity	k_w	0.598 W/(m · K)
Viscosity	μ_w	1.002×10^{-3} Pa · s
Prandtl number	Pr	7.01
Process flow rate	$\dot{V}$	0.50 L/min

Table 3: TEC module datasheet and back-calculated parameters.

Parameter	Symbol	Value	Source
Datasheet (at $T_h = 299.8$ K)			
Maximum cooling power	$Q_{\max}$	180 W	Datasheet
Maximum temperature drop	$\Delta T_{\max}$	60.0 K	Datasheet
Maximum voltage	$V_{\max}$	12.0 V	Datasheet
Maximum current	$I_{\max}$	15.0 A	Datasheet
Footprint	—	42.9 mm square (1-11/16")	Datasheet
Back-calculated (corrected voltage relation)			
Seebeck coefficient	$S_{p\text{-}n}$	0.054 58 V/K	Eqs. 1, 3
Electrical resistance	R_e	0.582 Ω	Eqs. 1, 3
Conduction resistance	R_t	0.458 K/W	Eq. 2
Figure of merit	$Z\bar{T}$ at 300 K	0.70	—
Number of modules	M	10	Design

Table 4: Cold-side thermal resistance budget (per module).

Component	Basis	Value [K/W]
Convection (water → pipe ID)	Re = 471 (laminar), Nu = 25.4	0.409
Pipe wall conduction (316L SS)	$\ln(D_o/D_i)/2\pi k_p L_{\text{eff}}$	0.033
Contact (pipe OD → TEC via Cu saddle)	Machined saddle + TIM	0.020
Total R_{cold}		**0.461**

Table 5: Hot-side liquid heat exchanger (per module).

Parameter	Symbol	Value
Coolant flow rate	$\dot{V}_{\text{hot}}$	8.0 L/min
Channel diameter	D_{ch}	5 mm
Block length	L_{block}	101.6 mm (4")
Block conduction	R_{block}	0.005 K/W
TIM resistance	R_{TIM}	0.015 K/W
Total	R_{sink}	0.042 K/W

Table 6: Operating conditions and design constraints.

Parameter	Symbol	Value
Cabin ambient range	T_{amb}	18 °C to 27 °C
Outlet target	T_{target}	$\leq$ 16 °C
Cabin dew point	T_{dew}	14.5 °C (nominal) / 22 °C (worst case)
Payload power budget	P_{avail}	2000 W at 28 V DC
Effective coupling length	L_{eff}	51.3 mm (footprint + axial spread)

4 Computed Resistances

At $\dot{V} = 0.50\,\text{L/min}$ in the 22.45 mm ID pipe:

$$v = 0.021\,\text{m/s}, \quad \text{Re} = 471 \text{ (laminar)} \tag{12}$$

$$\text{Gz} = \text{Re}\,\text{Pr}\,\frac{D_i}{L_{\text{eff}}} = 1444, \quad \text{Nu} = 25.4 \quad \text{(laminar developing-flow correlation)} \tag{13}$$

$$h = \frac{\text{Nu}\,k_w}{D_i} = 676\,\text{W/(m}^2\cdot\text{K)} \tag{14}$$

Wetted area per module:

$$A = \pi D_i L_{\text{eff}} = \pi \times 0.02245 \times 0.0513 = 3.62 \times 10^{-3}\,\text{m}^2 \tag{15}$$

$$R_{\text{conv}} = \frac{1}{hA} = 0.409\,\text{K/W}, \qquad R_{\text{pipe}} = \frac{\ln(D_o/D_i)}{2\pi k_p L_{\text{eff}}} = 0.033\,\text{K/W} \tag{16}$$

$$\boxed{R_{\text{cold}} = 0.409 + 0.033 + 0.020 = 0.461\,\text{K/W}} \tag{17}$$

The hot side carries 8 L/min of coolant through a 5 mm channel (Re = 33 800, turbulent):

$$\text{Nu} \approx 235, \quad h = 28\,090\,\text{W/(m}^2\cdot\text{K)}, \quad \boxed{R_{\text{sink}} = 0.042\,\text{K/W}} \tag{18}$$

Process mass flow: $\dot{m} = 0.0083\,\text{kg/s}$.

Cold-side geometry rationale. A machined copper water block with parallel internal channels would give a lower cold-side resistance ($R_{\text{cold}} \approx 0.286\,\text{K/W}$) but is incompatible with iodinated process water. The 316L stainless pipe with external copper saddle block gives $R_{\text{cold}} = 0.461\,\text{K/W}$ and requires ten modules to achieve the same outlet temperature, but is the only geometry consistent with the material compatibility requirement. The higher resistance is an accepted cost of iodine compatibility.

5 Results

5.1 Design Point Summary

Table 7: Design-point summary: 10 modules, 3/4" SS pipe, copper saddle, liquid HX hot side, 0.50 L/min. $\min T_2$ is the coldest TEC cold-face temperature.

T_{amb} [°C]	I_{min} [A]	T_{out} [°C]	P_{tot} [W]	COP	Q_{cool} [W]	$\min T_2$ [°C]
18.0	1.15	15.90	11	6.87	73.0	13.2
22.5	3.92	15.94	122	1.88	228.2	7.4
27.0	7.36	16.00	421	0.91	382.6	1.8

The 16 °C outlet target is met across all three evaluated ambient cases in the steady-state sequential model. At 18 °C and 22.5 °C, cold faces remain comfortably above freezing. At the 27 °C worst case the array draws 421 W at 7.36 A per module — within the 15 A I_{max} limit and well within the 2000 W payload budget — while maintaining a cold-face margin of 1.8 °C at the final module. The total heat rejection load on the coolant loop is $Q_{reject} = Q_{cool} + P_{elec} = 803.6$ W.

Table 8: Worst-case energy balance at $T_{amb} = 27$ °C.

Quantity	Expression	Value
Cooling from process water	$Q_{cool} = \sum q_{cold}$	382.6 W
TEC electrical input	$P_{tot} = \sum P_{elec}$	421 W
Heat rejected to coolant loop	Q_{reject}	803.6 W

5.2 Per-Module Detail (Worst Case)

Table 9: Per-module breakdown at $T_{amb} = 27$ °C, $I = 7.36$ A. Downstream modules pump less heat and exhibit lower COP as the water progressively cools. All cold faces remain above freezing; the tightest margin is 1.8 °C at module 10.

Mod.	T_{in} [°C]	T_{out} [°C]	q_{cold} [W]	P_{elec} [W]	COP	T_2 [°C]	T_1 [°C]
1	27.00	25.73	44.24	41.19	1.07	6.6	30.6
2	25.73	24.50	42.79	41.41	1.03	6.0	30.6
3	24.50	23.31	41.39	41.62	0.99	5.4	30.5
4	23.31	22.16	40.04	41.83	0.96	4.8	30.5
5	22.16	21.04	38.73	42.03	0.92	4.3	30.4
6	21.04	19.97	37.46	42.23	0.89	3.8	30.4
7	19.97	18.92	36.23	42.41	0.85	3.3	30.3
8	18.92	17.92	35.05	42.60	0.82	2.8	30.3
9	17.92	16.94	33.90	42.77	0.79	2.3	30.2
10	16.94	16.00	32.79	42.94	0.76	1.8	30.2
Total	27.00	16.00	**382.6**	**421.0**	**0.91**		

5.3 Condensation, Freezing Margin, and PID Control

At the 27 °C worst-case design point (7.36 A per module), the outlet water reaches 16 °C and the TEC cold faces range from 6.6 °C at module 1 to 1.8 °C at module 10. All cold faces remain above freezing, with the tightest margin of 1.8 K at module 10.

Two conditions persist regardless of the positive freeze margin. First, all cold faces are below the cabin dew point (14.5 °C nominal; 22 °C worst case at 75% RH), making the aerogel-insulated cold-side enclosure mandatory to prevent condensation. Second, the 1.8 K freeze margin at module 10 is the binding thermal-margin constraint: any increase in current beyond the design point, reduction in flow, or degraded hot-side performance risks driving that face below freezing.

A closed-loop PID controller modulates drive current to target the 14 °C to 16 °C outlet band. A per-module cold-face floor limiter ($T_{2,\text{floor}} = 1\,°\text{C}$, providing approximately a 1 K nominal margin above freezing prior to accounting for sensor uncertainty) overrides the PID if any cold face approaches the freeze threshold, taking absolute priority over the outlet loop. An outlet anti-condensation floor (14.5 °C) prevents the outlet PID from driving dispensed water below the downstream dew point. Under nominal steady-state conditions both constraints are satisfied simultaneously; hardware validation should confirm this margin is maintained across transient and off-nominal operating states.

5.3.1 Aerogel Insulation Thickness

The aerogel blanket was measured at $k_{\text{ins}} = 0.024\,\text{W/(m·K)}$ at 20 °C [3]. Using the steady-state conduction–convection balance at the limiting condition $T_{\text{surface}} = T_{\text{dew}}$:

$$L_{\text{req}} = \frac{k_{\text{ins}}}{h_{\text{ext}}} \cdot \frac{T_{\text{dew}} - T_{\text{inner}}}{T_{\infty} - T_{\text{dew}}} = \frac{0.024}{2.0} \cdot \frac{22 - 0}{27 - 22} = 52.8\,\text{mm} \tag{19}$$

Inputs: $h_{\text{ext}} = 2.0\,\text{W/(m}^2\cdot\text{K)}$ (conservative microgravity cabin), $T_{\text{inner}} = 0\,°\text{C}$ (worst-case cold face), $T_{\text{dew}} = 22\,°\text{C}$ (calculated from the 27°C dry-bulb, 75% RH worst-case cabin condition per NASA-STD-3001 [2]).

Selected thickness: 60 mm. Verification:

$$T_{\text{surface}} = \frac{h_{\text{ext}} T_{\infty} + (k_{\text{ins}}/L)\, T_{\text{inner}}}{h_{\text{ext}} + k_{\text{ins}}/L} = \frac{2.0 \times 27 + 0.400 \times 0}{2.400} = 22.50\,°\text{C} \tag{20}$$

Margin: 0.50 K above worst-case dew point. **PASS.** Under nominal cabin conditions (22.5°C, 50% RH, $T_{\text{dew}} \approx 12\,°\text{C}$), the margin is 6.75 K. Full derivation and both dew-point cases are tabulated in Appendix A.4.

5.4 Long-Duration Fouling Sensitivity

A 25–50% increase in R_{sink} models heat-exchanger fouling over the 1200-day Mars mission. The target remains achievable within the power budget throughout.

Table 10: Hot-side fouling sensitivity at $T_{\text{amb}} = 27\,°\text{C}$, $M = 10$. PID-compensated: current and power required to maintain 16 °C target.

Condition	R_{sink} [K/W]	I_{min} [A]	P_{tot} [W]	COP	$T_{1,\text{hot}}$ [°C]
Nominal	0.0423	7.38	423	0.91	31
+25% (fouled)	0.0529	7.57	446	0.86	32
+50% (degraded)	0.0635	7.79	474	0.81	33

A 50% increase in R_{sink} raises required current by approximately 0.4 A and total power by approximately 51 W (12%), while the hot junction rises only 2 K to 33 °C — all well within limits. The system remains feasible throughout the fouling range within the 2000 W payload budget. Small differences between the nominal fouling row and table 7 are due to solver tolerance and rounding.

5.5 Control Architecture

The outlet water temperature and the TEC cold-face temperatures are two distinct controlled quantities. Under the nominal steady-state design point all cold faces remain above freezing, but the tightest margin is only 1.8 K at module 10. Any increase in drive current beyond the design point, or degradation of hot-side performance, risks violating the freeze constraint. The cascade architecture below governs normal operation through the outlet PID while providing per-module floor limiters as protective overrides that take priority whenever any cold face approaches the freeze threshold.

5.5.1 Proposed Architecture: Cascade with Per-Module Floor Limiters

The control system uses three layers:

Layer 1 — Outer outlet PID. A proportional-integral-derivative controller with the outlet water temperature as the process variable and a per-module drive current reference as the output. The setpoint is 16 °C. This loop runs continuously and governs normal operation across the full ambient range.

Layer 2 — Per-module cold-face floor limiters. Each of the ten modules has a dedicated cold-face temperature sensor ($T_{2,k}$). If any $T_{2,k}$ falls below a defined floor (recommended: $T_{2,\text{floor}} = 1\,°\text{C}$, providing approximately a 1 K nominal margin above freezing prior to accounting for sensor uncertainty), that module's current driver clamps at the value that holds $T_{2,k} = T_{2,\text{floor}}$. This override takes absolute priority over the outer PID command. The clamped current for module k is solved implicitly from:

$$T_{2,k} = T_{\text{water,in,k}} - q_{\text{cold,k}}(I_k)\, R_{\text{cold}} = T_{2,\text{floor}} \quad \Rightarrow \quad I_k = I_{\text{clamp,k}} \tag{21}$$

Layer 3 — Outlet anti-condensation floor. The outlet water must also remain above the dew point of any downstream surfaces (14.5 °C nominal). If the outlet PID attempts to drive the outlet below this floor, the setpoint is clamped. This prevents the outlet water itself from being a condensation source in downstream lines.

5.5.2 Consequence at Worst-Case Ambient

Under nominal steady-state worst-case operation the floor limiters are not actively constraining: the design current of 7.36 A meets the outlet target while keeping all cold faces above freezing. The per-module limiter architecture therefore serves primarily as a protective override for transient conditions, degraded heat rejection, sensor uncertainty, or off-nominal ambient rather than as a continuously active constraint.

The per-module current architecture provides an additional advantage: upstream modules have warmer inlet water and larger cold-face margins and can run closer to full current, while downstream modules with tighter margins are limited independently. This distributes the cooling load more efficiently than a single common current command and improves fault tolerance.

5.5.3 Summary

Table 11: Control layer summary.

Layer	Variable	Mechanism	Priority
1	Outlet water temp	Outlet PID	Normal
2	Cold-face temp (per module)	Current clamp floor	Override (highest)
3	Outlet floor (anti-condensation)	Setpoint clamp	Override

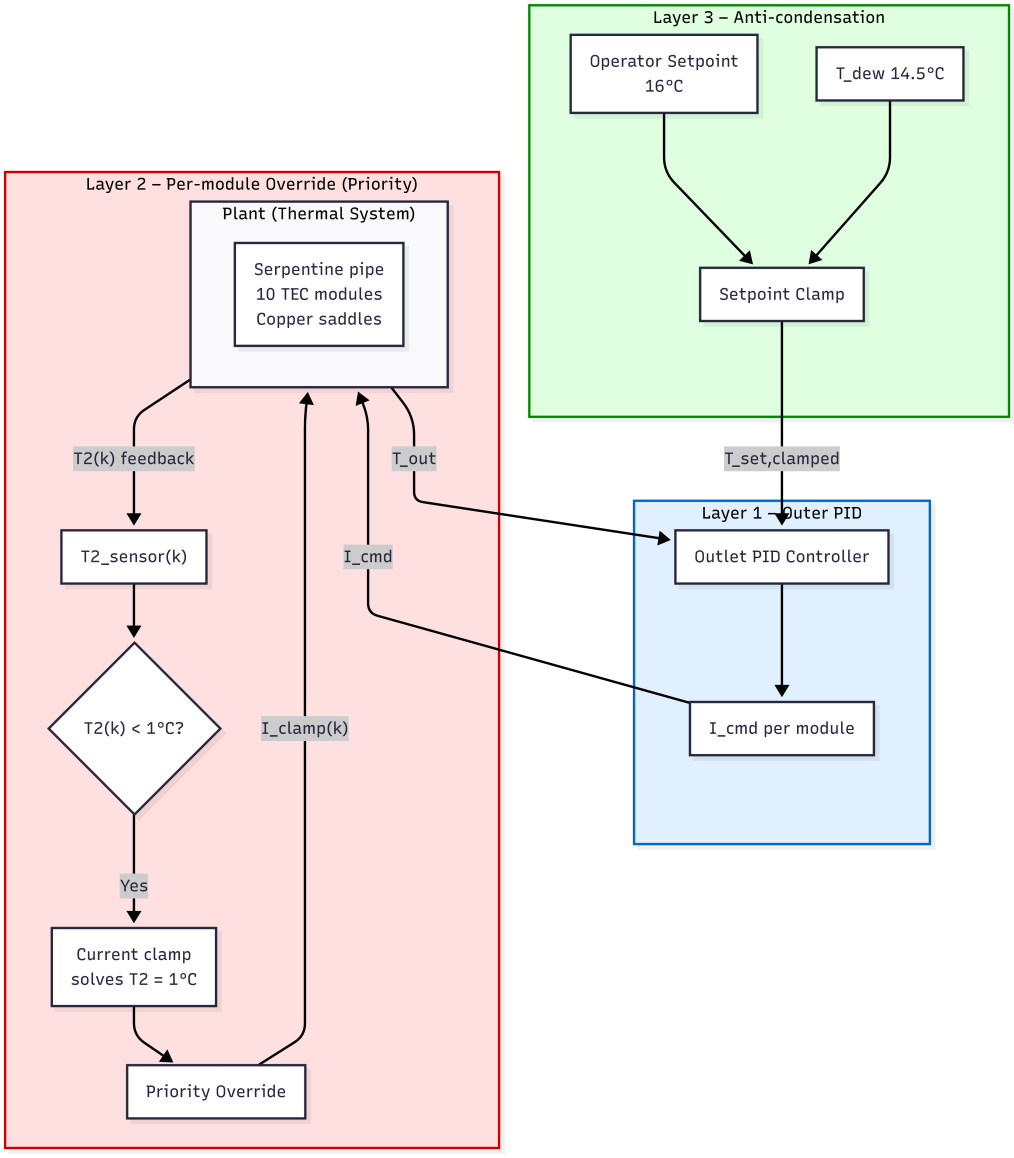

Figure 1: Cascade control architecture with per-module cold-face floor limiters. Layer 3 clamps the outlet setpoint above the condensation limit; Layer 2 overrides the PID command if any T_2 falls below 1 °C.

5.6 Figures

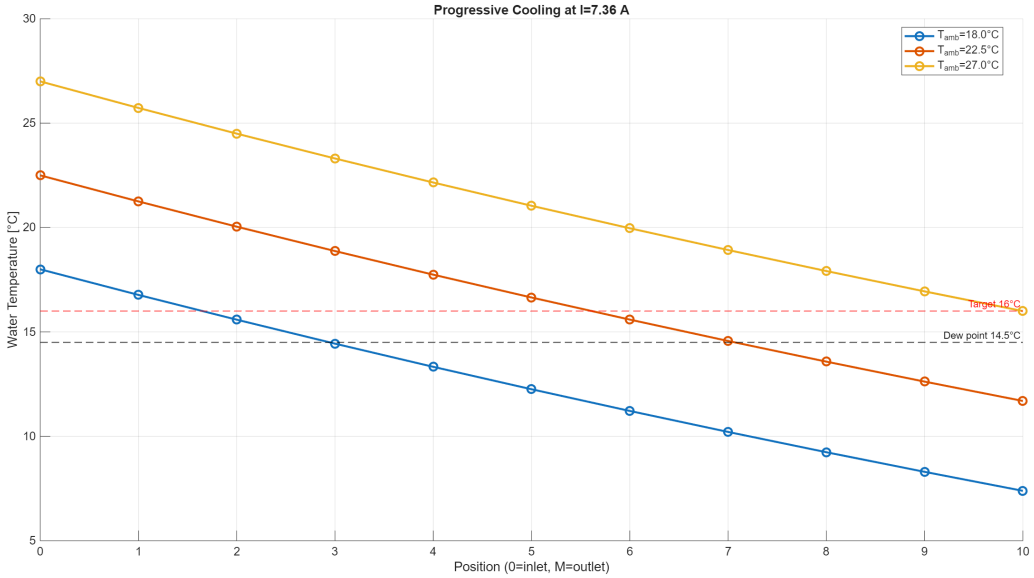

Figure 2: Progressive cooling profile at $I = 7.36\,\mathrm{A}$. Each step is one module; downstream steps shrink as water approaches target.

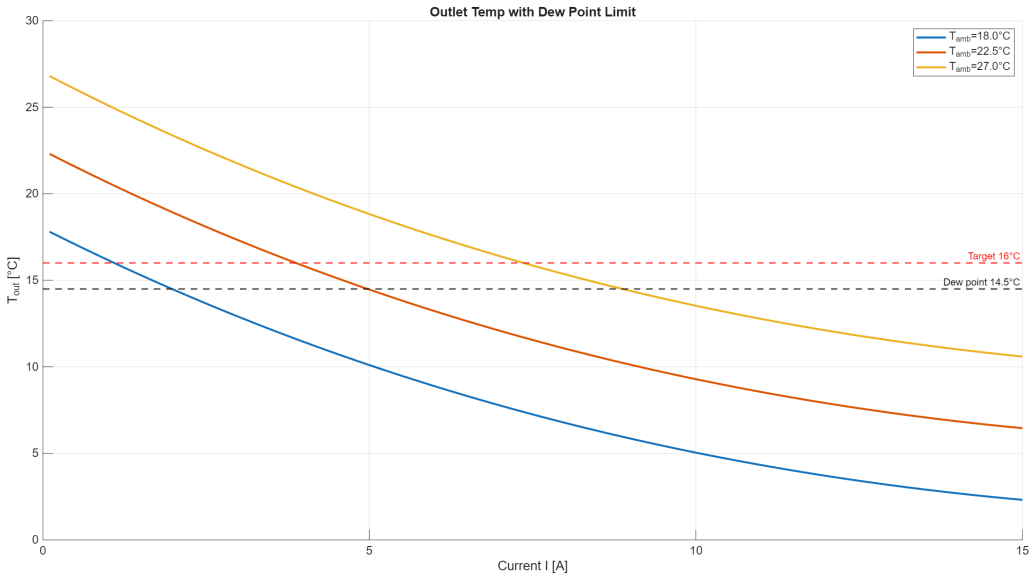

Figure 3: Outlet water temperature vs. per-module current with dew-point and target reference lines.

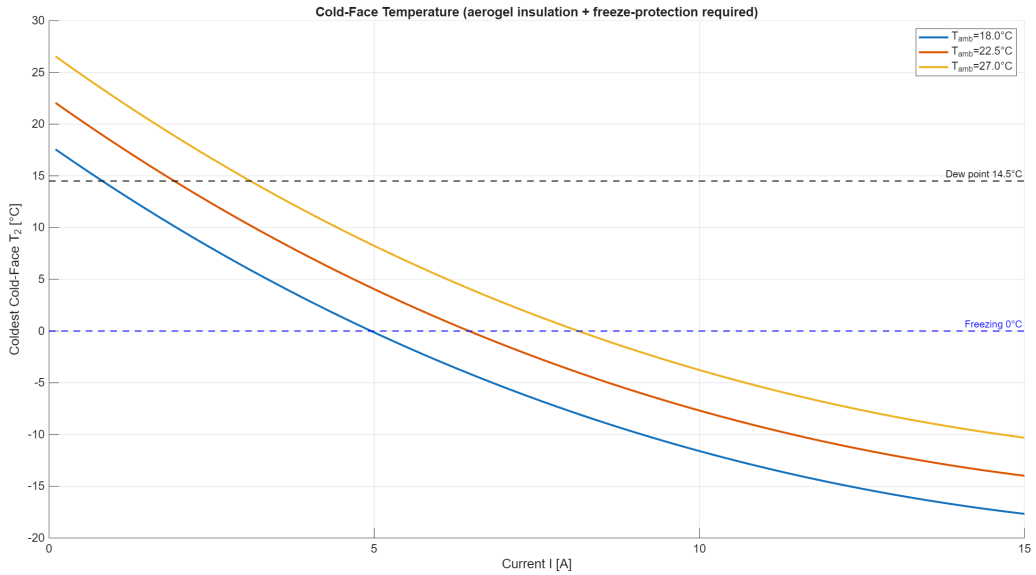

Figure 4: Coldest cold-face temperature (T_2, final module) vs. current. At the design operating point the cold face remains above freezing; aerogel insulation is required because all cold faces operate below the cabin dew point.

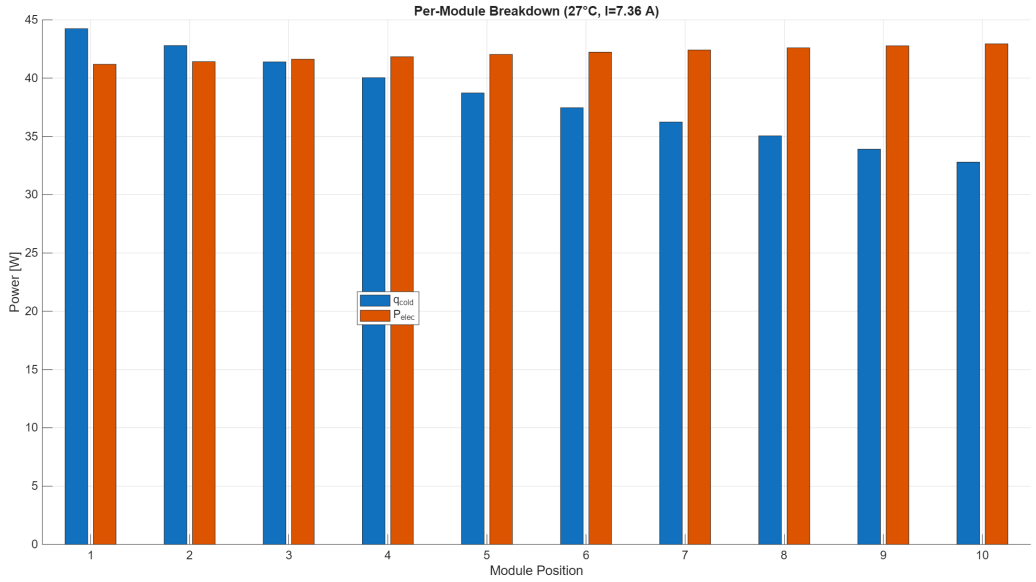

Figure 5: Per-module power breakdown at $T_{\mathrm{amb}} = 27\,^{\circ}\mathrm{C}$, $I = 7.36\,\mathrm{A}$. Cooling capacity decreases downstream while electrical power rises slightly.

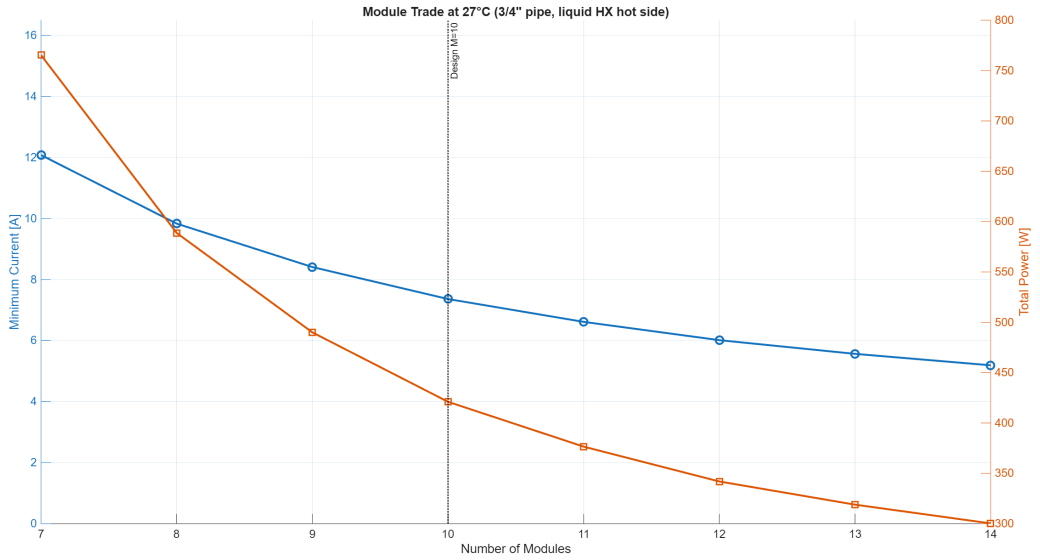

Figure 6: Module count trade at 27 °C. Fewer than 8 modules is not feasible with this pipe geometry; 10 modules gives a comfortable operating current margin.

6 Conclusions

The ten-module configuration with 3/4” stainless steel serpentine pipe, copper saddle blocks, and liquid heat-exchanger hot side meets the design envelope:

- 16 °C target met across the 18 °C to 27 °C ambient range in the steady-state sequential model.
- Worst-case current 7.36 A per module, within 15 A $I_{\max}$.
- Worst-case total TEC power 421 W, within 2000 W payload budget.
- Coolant loop heat rejection load: 803.6 W at worst case ($Q_{\text{cool}} + P_{\text{elec}} = 382.6 + 421.0$ W).
- Hot junction held near 31 °C by liquid HX, confirming the air-cooled sink is infeasible.
- 316L stainless steel pipe is the sole wetted material; copper is used only externally as a saddle block, preserving compatibility with iodinated water.
- Cold faces remain above freezing during nominal worst-case operation (minimum 1.8 °C at module 10); aerogel insulation (60 mm, $k = 0.024\,\text{W}/(\text{m}\cdot\text{K})$ measured) is mandatory for condensation control, and freeze-protection current limiting is retained as a protective feature for off-nominal conditions.
- Hot-side fouling of up to 50% R_{sink} increase is accommodated at 474 W total power, hot junction 33 °C.

6.1 Open Items

- **Control law validation:** The cascade architecture (outlet PID + per-module cold-face floor limiters) must be validated by transient simulation and hardware test. Although the steady-state model predicts positive freeze margin (1.8 °C at module 10) under nominal worst-case conditions, dynamic operation, flow transients, degraded heat rejection, or sensor uncertainty may reduce this margin.

- **Freeze-protection control law:** Validate the current-clamp logic and quantify outlet temperature response when the freeze floor becomes active under off-nominal conditions. The 1.8 °C nominal margin provides limited headroom against transients.
- **Saddle block geometry:** $R_{\text{contact}} = 0.020\,\text{K/W}$ is an estimate for a well-machined conforming saddle. Confirm by measurement or detailed FEA once saddle geometry is defined.
- **TEC parameter verification:** Back-calculated $R_e = 0.582\,\Omega$ and $Z\bar{T} = 0.70$ should be confirmed by bench V–I and calorimetric testing on the procured module.
- **Coolant loop closure:** The assumed 8 L/min coolant flow and $T_{\text{coolant,in}} = T_{\text{amb}}$ boundary condition must be closed out against the actual manifold, pump curve, and spacecraft thermal-control interface.
- **Conjugate heat transfer:** The lumped R_{cold} model does not resolve local channel-wall temperatures. A conjugate model or instrumented test is needed to confirm no ice forms at the saddle contact patch before the bulk water approaches freezing.

A Thermal Resistance Derivation

A.1 Cold-Side: Pipe Wall and Saddle Block

A.1.1 Internal Convection

The effective coupling length along the pipe for each TEC module is increased beyond the bare TEC footprint to account for axial heat spreading within the pipe wall:

$$L_{\text{eff}} = L_{\text{TEC}}+2t_w = 42.9+2(2.11) = 47.1\,\text{mm} \quad \text{(increased to 51.3 mm to account for axial spreading beyond th} \tag{22}$$

$$v = \frac{\dot{V}}{\frac{\pi}{4}D_i^2} = \frac{8.33\times10^{-6}}{\frac{\pi}{4}(0.02245)^2} = 0.021\,\text{m/s}, \qquad \text{Re} = \frac{998\times0.021\times0.02245}{1.002\times10^{-3}} = 471 \tag{23}$$

Laminar developing flow (Sieder–Tate type):

$$\text{Gz} = \text{Re}\,\text{Pr}\,\frac{D_i}{L_{\text{eff}}} = 471\times7.01\times\frac{0.02245}{0.0513} = 1444 \tag{24}$$

$$\text{Nu} = 25.4 \quad \text{(laminar developing-flow correlation)}, \qquad h = \frac{25.4\times0.598}{0.02245} = 676\,\text{W/(m}^2\cdot\text{K)} \tag{25}$$

$$A = \pi D_i L_{\text{eff}} = 3.62\times10^{-3}\,\text{m}^2, \qquad R_{\text{conv}} = \frac{1}{hA} = 0.409\,\text{K/W} \tag{26}$$

A.1.2 Pipe Wall Conduction

$$R_{\text{pipe}} = \frac{\ln(D_o/D_i)}{2\pi k_p L_{\text{eff}}} = \frac{\ln(26.67/22.45)}{2\pi\times16.3\times0.0513} = 0.033\,\text{K/W} \tag{27}$$

A.1.3 Contact Resistance (Copper Saddle Block)

The saddle block is machined to conform to the pipe OD, eliminating the line-contact geometry of a flat TEC pressed directly against a round pipe. With thermal interface material (TIM) at both interfaces (pipe OD to saddle, saddle to TEC face):

$$R_{\text{contact}} \approx 0.020\,\text{K/W} \quad \text{(vs. 0.050 K/W for bare flat-on-round contact)} \tag{28}$$

$$\boxed{R_{\text{cold}} = 0.409 + 0.033 + 0.020 = 0.461\,\text{K/W}} \tag{29}$$

A.2 Hot-Side: Liquid Heat Exchanger

High coolant flow (8 L/min) through a 5 mm channel, 101.6 mm long:

$$v = 6.79\,\text{m/s}, \quad \text{Re} = 33\,800 \text{ (turbulent)}, \quad \text{Nu} \approx 235 \tag{30}$$

$$h = 28\,090\,\text{W}/(\text{m}^2 \cdot \text{K}), \quad R_{\text{conv,hot}} = 0.022\,\text{K/W} \tag{31}$$

$$\boxed{R_{\text{sink}} = 0.022 + 0.005 + 0.015 = 0.042\,\text{K/W}} \tag{32}$$

A.3 Cold Water Dispense Time

For a single-pass system at steady state, fill time is $t = V/\dot{V}$. No heating-cycle delay applies; the TEC runs continuously.

Table 12: Cold water fill time [s] vs. volume and flow rate.

Volume [mL]	0.35 L/min	0.50 L/min (nominal)	0.65 L/min
25	4.3	3.0	2.3
50	8.6	6.0	4.6
100	17.1	12.0	9.2
150	25.7	18.0	13.8
200	34.3	24.0	18.5
250	42.9	30.0	23.1

The retained downstream volume (pipe run + UV chamber, ≈123.8 mL) must be purged before cold water reaches the nozzle, requiring approximately 11.4–21.2 s depending on flow rate. After standby this retained volume warms toward ambient with a time constant of approximately 68.5 min; a brief auto-purge on solenoid opening ensures cold delivery.

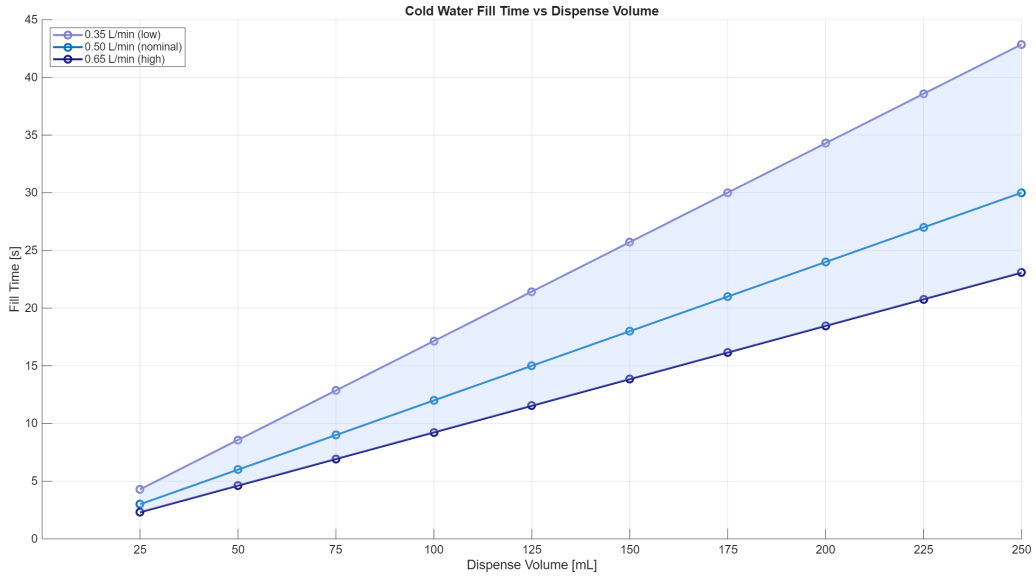

Figure 7: Cold water fill time vs. dispense volume. Shaded band shows flow-rate uncertainty from supply pressure variation.

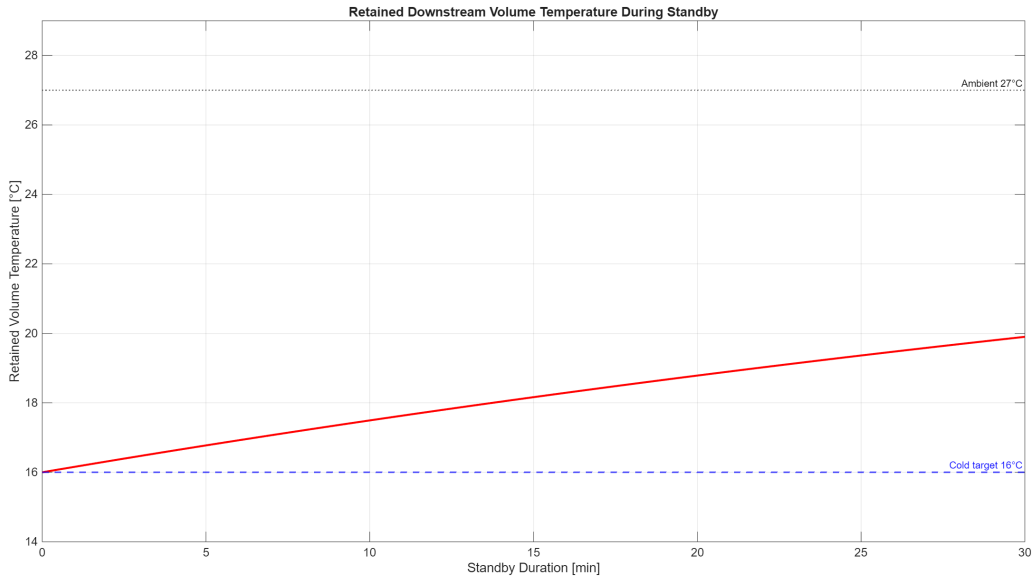

Figure 8: Retained downstream volume temperature during standby. Time constant $\tau \approx 68.5\,\text{min}$; auto-purge on solenoid opening ensures cold delivery after extended standby.

A.4 Aerogel Insulation Sizing

The thermal conductivity of the aerogel blanket was measured at $0.024\,\text{W}/(\text{m}\cdot\text{K})$ at $20\,^\circ\text{C}$ [3]. The lower value of $0.015\,\text{W}/(\text{m}\cdot\text{K})$ sometimes cited in literature applies to pure silica aerogel monoliths in idealized or dry conditions; blanket-form aerogel at ambient atmospheric pressure and humidity measures higher. The measured value is used throughout.

$$L_{\text{req}} = \frac{k}{h} \cdot \frac{T_{\text{dew}} - T_{\text{inner}}}{T_\infty - T_{\text{dew}}} \tag{33}$$

Table 13: Aerogel insulation sizing inputs and results at two dew-point conditions.

Parameter	Worst case	Nominal
Cabin dry-bulb T_∞	$27\,^\circ\text{C}$	$22.5\,^\circ\text{C}$
Relative humidity	75%	50%
Dew point T_{dew}	$22\,^\circ\text{C}$	$12\,^\circ\text{C}$
Inner surface T_{inner}	$0\,^\circ\text{C}$ (worst-case cold face)	
Aerogel conductivity k	$0.024\,\text{W}/(\text{m}\cdot\text{K})$ (measured)	
Convection h_{ext}	$2.0\,\text{W}/(\text{m}^2\cdot\text{K})$ (conservative)	
Minimum required thickness L_{req}	52.8 mm	13.7 mm
Selected thickness	60 mm	
Outer surface temperature	$22.50\,^\circ\text{C}$	$18.75\,^\circ\text{C}$
Condensation margin	0.50 K **PASS**	6.75 K **PASS**

The selected 60 mm thickness is required to cover the worst-case humidity condition (27°C, 75% RH). Under nominal cabin conditions the 60 mm selection provides a 6.75 K margin, confirming it is conservative relative to the most probable operating environment.

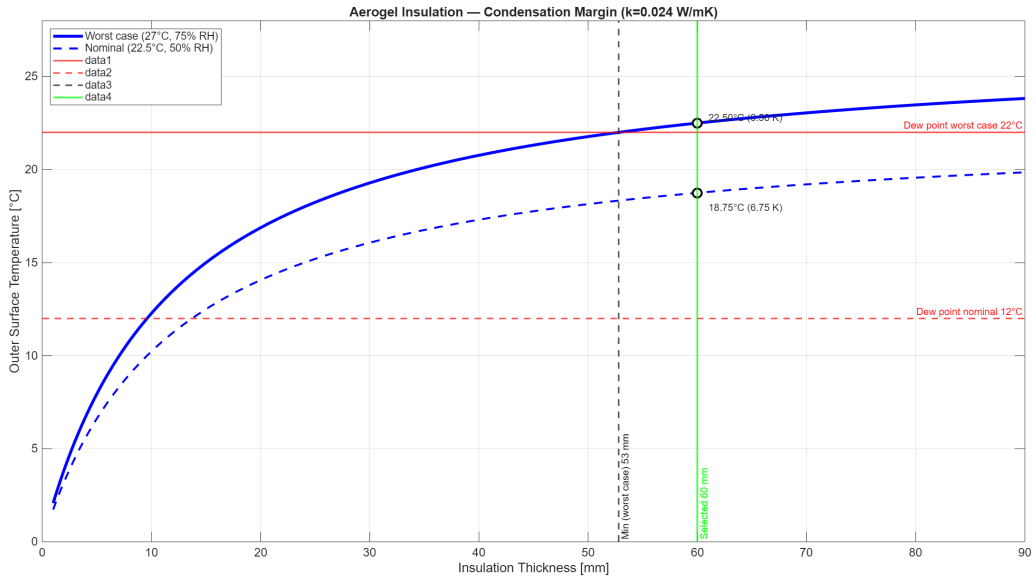

Figure 9: Aerogel outer surface temperature vs. thickness at worst-case (27°C, 75% RH) and nominal (22.5°C, 50% RH) cabin conditions. Selected 60 mm provides 0.50 K margin at worst-case dew point (22 °C) and 6.75 K at nominal dew point (12 °C).

A.5 ISS PWD Heater Power Estimate

The ISS PWD requirement is to supply up to 2.0 L of hot water at 65 °C to 93 °C every 30 min [5]. A first-law energy balance provides an estimate of the minimum continuous heater power required.

Assume:

$$V = 2.0\,\mathrm{L} \tag{34}$$

$$\rho_w \approx 1000\,\mathrm{kg/m^3} \tag{35}$$

$$m = \rho_w V \approx 2.0\,\mathrm{kg} \tag{36}$$

$$T_{\mathrm{in}} = 18\,^{\circ}\mathrm{C} \tag{37}$$

$$T_{\mathrm{out}} = 93\,^{\circ}\mathrm{C} \tag{38}$$

$$\Delta T = T_{\mathrm{out}} - T_{\mathrm{in}} = 75\,\mathrm{K} \tag{39}$$

$$c_{p,w} = 4182\,\mathrm{J/(kg \cdot K)} \tag{40}$$

Required thermal energy:

$$Q = mc_p\,\Delta T = (2.0\,\mathrm{kg})(4182\,\mathrm{J/(kg \cdot K)})(75\,\mathrm{K}) = 6.27 \times 10^5\,\mathrm{J} \tag{41}$$

Delivered over 30 min ($t = 1800\,\mathrm{s}$), the minimum continuous thermal power is:

$$P_{\mathrm{heater}} = \frac{Q}{t} = \frac{6.27 \times 10^5\,\mathrm{J}}{1800\,\mathrm{s}} \approx 350\,\mathrm{W} \tag{42}$$

$$\boxed{P_{\mathrm{heater,min}} \approx 350\,\mathrm{W}} \tag{43}$$

Real electrical heater demand will exceed this minimum due to thermal losses, heater inefficiency, tubing thermal mass, startup transients, and control margin. The practical electrical load is therefore estimated at several hundred watts above the 350 W floor. For the P.H.A.T. power budget, a conservative worst-case concurrent load is the TEC array (421 W) plus the heritage heater operating simultaneously. The exact heater electrical rating should be confirmed against Shaw & Barreda [5] or ISS operational documentation.

A.6 System Mass Estimate

A bottom-up mass estimate is provided in Table 14 based on component datasheets, catalog specifications, and engineering estimates. The ISS PWD heritage core mass is not directly stated in available published sources; a placeholder of 16 kg is used for cost estimation, consistent with the system occupying two Shuttle Middeck lockers [5] and comparable rack-scale life-support hardware. This figure should be confirmed against ISS PWD programme documentation before detailed design. All cold-loop line items carry preliminary-design uncertainty of ±20–30%; a verified mass budget requires a completed CAD model and hardware procurement, both planned for the 2026–2027 component testing phase.

The coolant loop pump, manifold, and supply tubing interface with the spacecraft Active Thermal Control System (ATCS) and are *not* included in the P.H.A.T. mass budget. A 15% structural margin is applied to the cold-loop subtotal to account for brackets, fasteners, and miscellaneous hardware not itemised below.

Table 14: P.H.A.T. system mass estimate. Heritage core value is a placeholder for cost estimation pending source verification. Cold-loop line items carry ±20–30% preliminary-design uncertainty; 15% structural margin applied to cold-loop subtotal.

Component	**Basis**	**Est. mass (kg)**
ISS PWD heritage core (heater, valves, filters, structure)	Placeholder for cost estimation; not confirmed in published sources [5]	16.0
10× TEC modules (180 W class)	Datasheet (TEC1-12715, 50 g each)	0.5
3/4" Sch. 10 316L SS serpentine pipe, est. 1.5 m	Catalog: 1.63 kg/m	0.9
10× copper saddle blocks	CAD estimate, 200 g each	2.0
10× liquid heat-exchanger blocks	Engineering estimate, 300 g each	3.0
Aerogel insulation enclosure	Bulk density ≈ 5 kg/m^3, est. 0.008 m^3	0.5
Solenoid valves, check valves, fittings (14 items)	Catalog: ≈ 200 g each	2.8
Electronics, wiring, PLC	Engineering estimate	2.0
Structure, mounting, miscellaneous	15% margin on cold-loop subtotal	2.3
Cold-loop subtotal		**14.0**
Heritage core (placeholder)	*pending verification*	**16.0**
Total P.H.A.T. (placeholder)	*pending verification*	**30.0**

The cold-loop addition is estimated at approximately 14.0 kg. A mass reduction trade focused on the heat-exchanger blocks and structural elements is recommended during detailed design, as these represent the largest discretionary mass items in the cold-loop subtotal.

References

[1] Bergman, T. L. and Incropera, F. P. (2011) *Introduction to Heat Transfer*. John Wiley & Sons, Hoboken.

[2] National Aeronautics and Space Administration (NASA), "NASA-STD-3001, Volume 2: Human Factors, Habitability and Environmental Health," Revision D, Office of the Chief Health and Medical Officer, 2023. Available: https://www.nasa.gov/ochmo/human-spaceflight-and-aviation-standards/

[3] Thermtest, "Aerogel Thermal Conductivity Using the Heat Flow Meter." Available: https://thermtest.com/application/aerogel-thermal-conductivity-hfm

[4] Mudgett, P., Flanagan, D., Schultz, J., and Sauer, R., "Depletion of Biocidal Iodine in a Stainless Steel Water System," *SAE Technical Paper* 941391, 1994. Available: https://doi.org/10.4271/941391

[5] Shaw, L. and Barreda, J., "International Space Station USOS Potable Water Dispenser Development," NASA Lyndon B. Johnson Space Center, 2008. Available: https://ntrs.nasa.gov/api/citations/20080013432/downloads/20080013432.pdf

[6] Maryatt, B. W., "Lessons Learned for the International Space Station Potable Water Dispenser," 48th International Conference on Environmental Systems, ICES-2018-114, 2019. Available: https://ttu-ir.tdl.org/server/api/core/bitstreams/028fd2b1-34ca-4dac-be77-7457a31470a0/content

Crew Systems

Cost Phase	FY2015 $M
Non-Recurring	$ 4.8
Design & Development	$ 3.6
System Test Hardware	$ 1.3
Flight Unit	$ 1.0
Recurring	$ 1.9
Non-Allocated	$ -
Operations	$ -
TOTAL	$ 6.8

INPUTS

Calculation Mode: Input Sensitivity/Uncertainty Only

Active Case: Case 1

Select Subsystem: Crew Systems

Crew Systems DD (v2.4 CASTS)

CER Inputs	Point Estimate	Case 1	Case 2	Input Dist.
Weight Per Unit (lbs)	35	74		
Adjustment Factor Type	Analogy			
Direct Input Factor		1.089		
Analogous Adjustment Factor	0.572	**0.572**	0.572	0.572

Crew Systems FU (v2.4 CASTS)

CER Inputs	Point Estimate	Case 1	Case 2	Input Dist.
Weight Per Unit (lbs)	35	74	0	0
Adjustment Factor Type	Analogy			
Direct Input Factor		1.089		
Analogous Adjustment Factor	0.804	**0.804**	0.804	0.804

CER Uncertainty & Allocations

Distribution for CER Uncertainty	Distribution	CER DoF
Crew Systems DD (v2.4 CASTS)	#CERDist	16
Crew Systems FU (v2.4 CASTS)	#CERDist	16

Allocation of CER Output	Non-Rec. %	Rec. %	Total
Crew Systems DD (v2.4 CASTS)	100%	0%	100%
Crew Systems FU (v2.4 CASTS)	0%	100%	100%

Other Inputs

Qty Next Higher Assembly	1
STH Quantity	1
STH Toggle	Direct Input
Direct Input Flight Unit %	130%
Total Number of Flights	2
Flight Rate Per Year	0.2
Learning Theory Type	Unit (Crawford)
Learning Curve Slope	100%
Production Start Unit	1
Production Rate %	100%

Analogous Adjustment Factors

?	Mission / Item	WBS Item	D&D	Fit Unit
	Apollo CSM	Crew Systems	2.9072	0.4605
	Apollo CSM	Displays & Controls	22.7689	7.0807
	Apollo CSM	ECLS	9.8718	3.2790
	Apollo LM	Crew Provisions Displays	13.7311	2.6055
	Apollo LM	Environ Control Life Supt	10.9381	3.6791
	ISS	Oxy Gen Sys	0.6831	0.9238
X	ISS	Water Recov Sys	0.5719	0.8038
	Orbiter	.1 ATMOS	0.9442	1.2272
	Orbiter	.2 LIFE SPT	0.5794	0.9204
	Orbiter	.3 THERMAL	0.6209	0.6640
	Orbiter	.4 AIRLOCK	0.5316	3.9762
	Orbiter	Orbiter ECLSS	0.7557	0.7839
	Orion	ACTS	1.3100	0.9274
	Orion	AVS	3.4679	1.3375
	Orion	Crew Systems	0.2355	0.0611
	Orion	Displays & Controls	0.4725	0.9560
	Orion	FDS	1.4847	0.9647
	Orion	FSI	0.5382	0.5263
	Orion	Orion CM+SM ECLSS	1.9266	0.6260
	Orion	PCS	2.1650	0.3667
	Orion	SM Radiators	3.3051	1.7755
	Orion	Tubing	0.3499	0.2027
	Orion	WMS	0.7209	0.3008
	Skylab	Spacelab ECLSS	1.3491	1.7568
	Skylab Airlock	Airlock ECS	20.7583	11.1512
	Skylab OWS	Orb Work Shop Cabin Atmos	0.2660	0.1793
	Skylab OWS	Orb Work Shop Crew Sys	0.1796	0.0998
	Spacelab	ECLS/ECLS - Long Module	1.3035	2.3135
	Spacelab	ECLS/TC-Long Module	1.7069	2.5291
	Spacelab	ECLS/TC-Pallet	1.3916	2.1396
	Spacelab	Igloo-Pallet	0.6988	1.4429
	Spacelab	SAM-Displays in Orbiter	0.1739	0.3763

Calculated Adjustment Factor: 0.5719 | 0.8038

DETAILED CER CALCULATIONS

Crew Systems DD (v2.4 CASTS)

	FY2015 $M	FY2015 $M		
Crew Systems DD (v2.4 CASTS)	$ 6.288	$ 6.288	Uncertainty Adjusted Prediction	#VALUE!
Weight Per Unit (lbs)	74	pounds, >0	SSE Adjusted	0.735
	0		Adjustment Factor	1.082
	0		SEE	0.679
	0		T-distribution	#CER1Dist
	0		Degrees of Freedom	16
	0		Regression Type	Log-linear regression

Selected Adjustment Factor: 0.572

Adjusted CER Output	FY2015 $M
	$ 3.596

Crew Systems FU (v2.4 CASTS)

	FY2015 $M	FY2015 $M		
Crew Systems FU (v2.4 CASTS)	$ 1.198	$ 1.198	Uncertainty Adjusted Prediction	#VALUE!
Weight Per Unit (lbs)	74	pounds, >0	SSE Adjusted	0.868
	0		Adjustment Factor	1.082
	0		SEE	0.802
	0		T-distribution	#CER2Dist
	0		Degrees of Freedom	16
	0		Regression Type	Log-linear regression

Selected Adjustment Factor: 0.804

Adjusted CER Output	FY2015 $M
	$ 0.963

Allocations of CER Output

	FY2015 $M
Non-Recurring / Development Estimate	$ 3.60
Recurring / Flight Unit Estimate	$ 0.96

TOTAL COST CALCULATIONS

Inputs (Linked)

Qty Next Higher Assembly	1	Learning Theory Type	Unit (Crawford)
STH Quantity	1	Learning Curve Slope	100%
STH Toggle	Direct Input	Learning Exponent	0.000
Direct Input STH Factor	130%	Learning Exponent + 1	1.000
Production Start Unit	1	Production Rate %	100%
Total Number of Flights	2	Production Rate Exponent	0.000
Flight Rate Per Year	0.2	Production Rate Exponent + 1	1.000
Total Subsystem Quantity Produced	2		
Production Rate Per Year	0.2		
Number of Production Years	10		

Flight Unit & Systems Test Hardware Calculations

STH % CER	2.312686463	Unit (Crawford)	CumAvg (Wright)
Flight Unit Cost (FY2015 $M)	$ 0.963	Fit Unit Total Cost Multiplier	1.000	1.000
FY2015 $M to FY2015 $M	1.000	Fit Unit Avg Unit Cost Multiplier	1.000	1.000
Selected STH Factor	**1.300**			
Selected Flight Unit Factor	**1.000**			

Recurring Production

Recurring Cost Calculation (Traditional)

Year	Cum. Units	Learning Effects	Prod. Qty/Yr	Rec. Prod $/Yr
1	0.2	$ 0.19	0.2	$ 0.19
2	0.4	$ 0.19	0.2	$ 0.19
3	0.6	$ 0.19	0.2	$ 0.19
4	0.8	$ 0.19	0.2	$ 0.19
5	1	$ 0.19	0.2	$ 0.19
6	1.2	$ 0.19	0.2	$ 0.19
7	1.4	$ 0.19	0.2	$ 0.19
8	1.6	$ 0.19	0.2	$ 0.19
9	1.8	$ 0.19	0.2	$ 0.19
10	2	$ 0.19	0.2	$ 0.19
11	2	$ -	0	$ -
12	2	$ -	0	$ -
13	2	$ -	0	$ -
14	2	$ -	0	$ -
15	2	$ -	0	$ -
16	2	$ -	0	$ -
17	2	$ -	0	$ -
18	2	$ -	0	$ -
19	2	$ -	0	$ -
20	2	$ -	0	$ -
			2	$ 1.93 FY2015 $M

Fixed/Variable Calculation

FY2015 $M	
T1,1	$ 0.963

Qty/Yr	Cost per Unit	Cost per Year
2	$ 0.96	$ 1.93
4	$ 0.96	$ 3.85
6	$ 0.96	$ 5.78
12	$ 0.96	$ 11.56

Variable Cost per Unit	$ 0.96
Fixed Cost per Year	$ -

Year	F/V Prod. $/Yr	RC vs. F/V
1	$ 0.19	1.000
2	$ 0.19	1.000
3	$ 0.19	1.000
4	$ 0.19	1.000
5	$ 0.19	1.000
6	$ 0.19	1.000
7	$ 0.19	1.000
8	$ 0.19	1.000
9	$ 0.19	1.000
10	$ 0.19	1.000
11	$ -	0.000
12	$ -	0.000
13	$ -	0.000
14	$ -	0.000
15	$ -	0.000
16	$ -	0.000
17	$ -	0.000
18	$ -	0.000
19	$ -	0.000
20	$ -	0.000
	$ 1.93	FY2015 $M
	Cumulative Diff	*0*
	% Diff	*0%*

Results

	FY2015 $M
Design & Development Cost	$ 3.596
System Test Hardware Cost	$ 1.252
Flight Unit Cost	$ 0.963
Total Production Cost	$ 1.926
Average Cost per Unit	$ 0.963
Average Cost per Flight	$ 0.963